BA, which is responsible to a β3-adrenergic receptor agonist, has also been generated from human multipotent adipose-derived stem cells by chronic treatment with thiazolidinediones (Elabd et al., 2009). The merit of our system is that it does not require preparation of human specimen materials but utilizes hPSCs, which are capable of unlimited expansion in vitro.

One of the main findings of our research is that HC composed of KITLG, IL6, FLT3LG, and VEGF is essential for BA differentiation of hPSCs. Although BMP7 plays an important role in BA differentiation of hPSC (Figure S2) as reported in murine cases (Tseng et al., 2008), HC is indispensable for BA differentiation of hPSCs (Figure 1D). It is known that VEGF is synthesized in rodent BAT (Asano et al., 1997; Tonello et al., 1999), promoting the angiogenesis within BAT. Moreover, IL6 is reportedly secreted from cultured human BM adipocytes (Laharrague et al., 2000). Our findings imply that VEGF and IL6, together with KITLG and FLT3LG, work as fundamental autocrine or paracrine factors to promote BA differentiation.

Compatible to the finding by Sellayah et al. (Sellayah et al., 2011), the inhibitor analyses demonstrated the involvement of p38 MAPK signaling, but not of MEK signaling, in BA differentiation of hESC (Figures 5E–5G). However, distinct findings were obtained from the case of hiPSCs, in which MEK signaling played a role in BA differentiation (Figure 5E–5G). At this moment, the basis for the difference in the effects of identical inhibitors between hESCs and hiPSCs remains elusive. It may be related to the difference in the genetic background of pluripotent stem cell lines, reflecting the individual difference of the "donor" or the difference in the type of pluripotent stem cells or both. Further investigations are required to obtain the whole picture of the molecular basis for BA differentiation of hPSCs.

By providing high-purity human BA and WA materials, we demonstrated the differential effects on metabolic regulation between BA and WA: BA improves while WA deteriorates glucose metabolism. Because those effects were confirmed by a short-term assay without body weight changes and also because the effects of BA and WA on lipid metabolism were similar, the beneficial effect of BA on glucose metabolism is not a secondary consequence of general metabolic improvement. Conventional subcutaneous fat transplantation experiments were not able to distinguish the effect of BA from that of WA, because subcutaneous fat tissues contain both WA and BA. Thus, our system will provide a unique tool for the research of BA in regard to glucose metabolism.

Another surprising finding is the functional link between BA and hematopoiesis. We showed that hPSCdBAs serve as a stroma for MPCs. In contrast to the "niche" for HSCs, which is composed of immature osteoblasts and sinusoidal endothelial cells, the "stroma" for committed HPCs remains a mystery. The only report showing the characteristic of such stroma was a study by Dexter et al. (Dexter et al., 1977), in which BM fat cells with multilocular lipid droplets attached by mitochondria were identified as a stroma for CFU-S. Our results indicating that (1) hPSCdBAs express various hematopoietic cytokines in response to β-adrenergic receptor stimuli, (2) hPSCdBAs promote myelopoiesis of human cord blood $CD34^+$ cells, and (3) β-adrenergic receptor stimuli accelerate the recovery from 5-FU-mediated myelosuppression together show that BM-BAT serves as a stroma for MPCs. Among those, the third finding is particularly important because it illustrates a very feasible way to shorten the period of myelosuppression, the major side effect of intensive chemotherapy for progressive cancers.

The PET-CT results of young healthy volunteers, together with gene expression analyses of human BM specimen and histological examinations of murine vertebral BM samples, strongly suggest the existence of active BAT in vertebral BM in mammals. Because classical BAT is derived from *Myf5*-positive myoblastic cells (Seale et al., 2008) and because *Myf5*-positive cells emerge at the juxtaspinal, prospectively paravertebral, regions within somites (Cossu et al., 1996; Braun and Arnold, 1996), the existence of BA in vertebral BM seems reasonable. Because the major portions of vertebrae are composed of trabecular bones, which are the sites of active hematopoiesis, and the vertebral marrow is the last reserve site for hematopoietic activity in aged individuals (Tanaka and Inoue, 1976), the hematopoietic microenvironment of vertebral BM may bear a unique character. Further investigation will elucidate the whole picture of HPC regulation.

Our system, providing highly functional hiPSCdBA, may open a new avenue to the therapy for obesity. However, we have found that BA differentiation efficiencies substantially differ among hiPSC lines (data not shown), as reported in the case of pancreatic β cell differentiation of hESCs (Osafune et al., 2008). For clinical application, selection of appropriate lines of hiPSCs will be as important as sophisticating the whole differentiation process into good manufacturing practice levels.

EXPERIMENTAL PROCEDURES

Establishment of hiPSCs and Provision of hESCs

SeV-iPS cells were established from human neonatal fibroblast or human umbilical vein endothelial cells by introducing Yamanaka's four factors using CytoTune-iPS ver.1.0 (DNAVEC Corp) (Figure S7). Transgenes were eliminated by a 39þC heat treatment for 5 days. A hESC line (KhES-3) was generously provided by the Institute for Frontier Medical Science, Kyoto University (Suemori et al., 2006).

A Directed Differentiation of hESCs/hiPSCs into Functional BA

hESCs or hiPSCs were cultured in a 6 cm low-attachment culture dish using a serum-free differentiation medium composed of 1:1 ratio of IMDM (I3390, Sigma Chemical Co.) and Ham's F12 (087-08335, WAKO Pure Chemical Industries), 5 mg/ml bovine serum albumin (A802, Sigma Chemical Co.), 1:100 synthetic lipids (GIBCO #11905-031, Life Technologies, Inc.), 450 μM α- monothioglycerol (207-09232, WAKO Pure Chemical Industries), 1:100 insulin-transferrin-selenium (ITS-A, Life Technologies, Inc.), 2 mM Glutamax II (GIBCO #35050-061, Life Technologies, Inc.), 5% protein-free hybridoma mix (PFHMII, GIBCO #12040-077, Life Technologies, Inc.), 50 μg/ml ascorbic acid-2-phosphate (Sigma, A-8960), and the hematopoietic cytokine cocktail I (5 ng/ml IGF-II, 20 ng/ml BMP4, 5 ng/ml VEGFA, 20 ng/ml KITLG, 2.5 ng/ml FLT3LG, 2.5 ng/ml IL-6) for 8 days to form spheres. The

immunostaining using an anti-UCP1 antibody (I) and anti-human HLA-A,B,C antibody (J) at day 7. Arrowheads in (H) indicate microvasculatures. Scale bars, 50 μm.

(K–M) Mice were transplanted with hMSCdWAs alone or together with hESCdBA, and OGTT was performed. Fasting blood glucose levels (K), HOMA-IR (L), and blood glucose values after oral glucose loading (M) are shown. The error bars in (A), (B), (D)–(G), (K), (L), and (M) represent average ± SD.

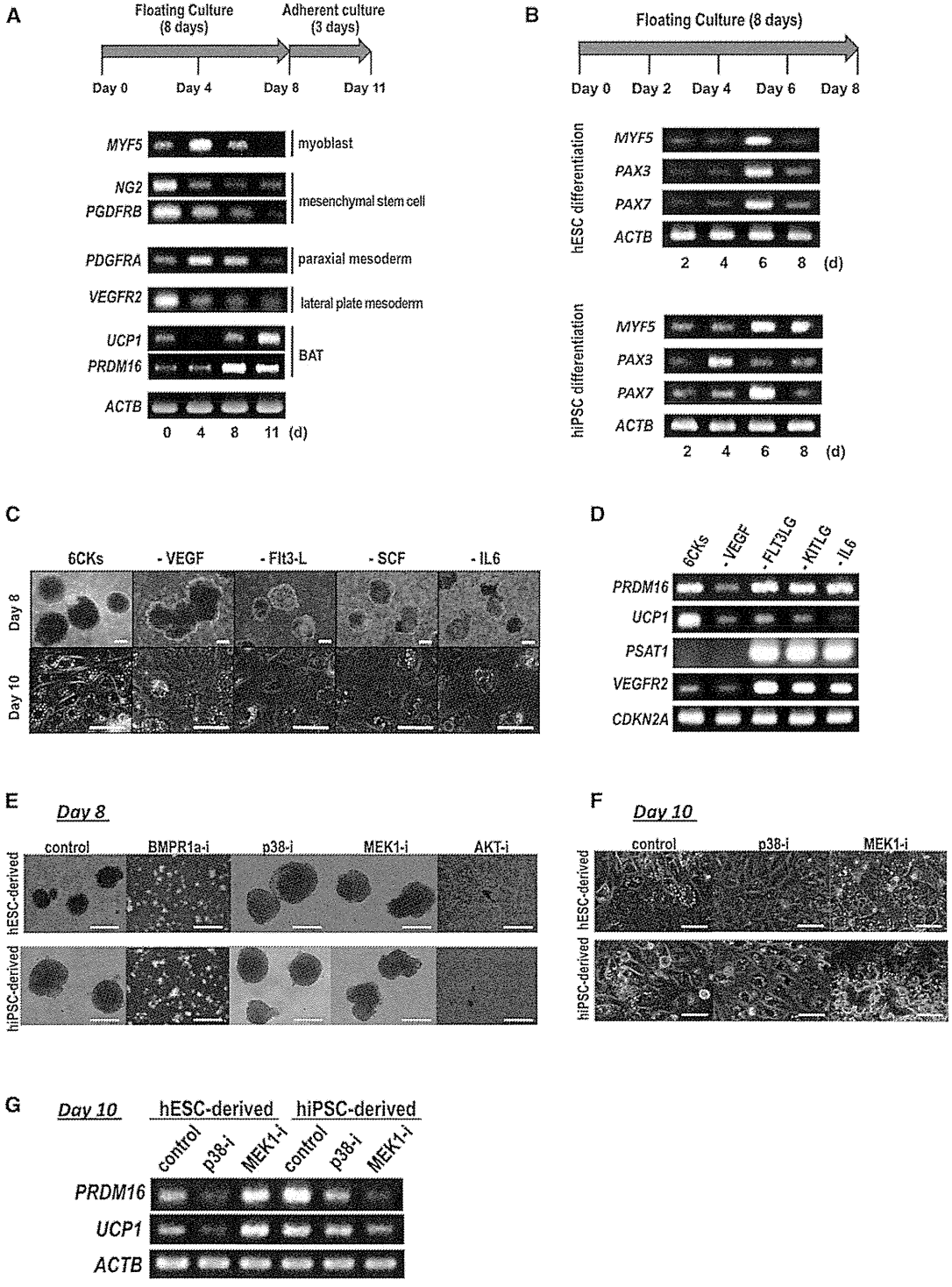

Figure 5. Signals Involved in BA Differentiation

(A) Developmental marker expression was examined by RT-PCR during BA differentiation of hESCs. Similar results were obtained regarding hiPSCs (data not shown).

(B) Myoblastic marker expressions were determined by RT-PCR during floating culture.

(C and D) The role of each cytokine was evaluated by morphological examinations (C) and RT-PCR (D). Scale bar, 100 μm (upper panels); and scale bar, 150 μm (lower panels).

(E–G) Inhibitor analyses. BA differentiation was performed in the presence of inhibitors of BMPR1a, p38 MAPK, MEK1, or AKT as indicated. Phase contrast micrographs of the spheres at day 8 (scale bar, 200 μm) (E) and those of BA at day 10 (scale bar, 50 μm) (F) were shown. Expressions of *UCP1* and *PRDM16* were determined at day 10 by RT-PCR (G).

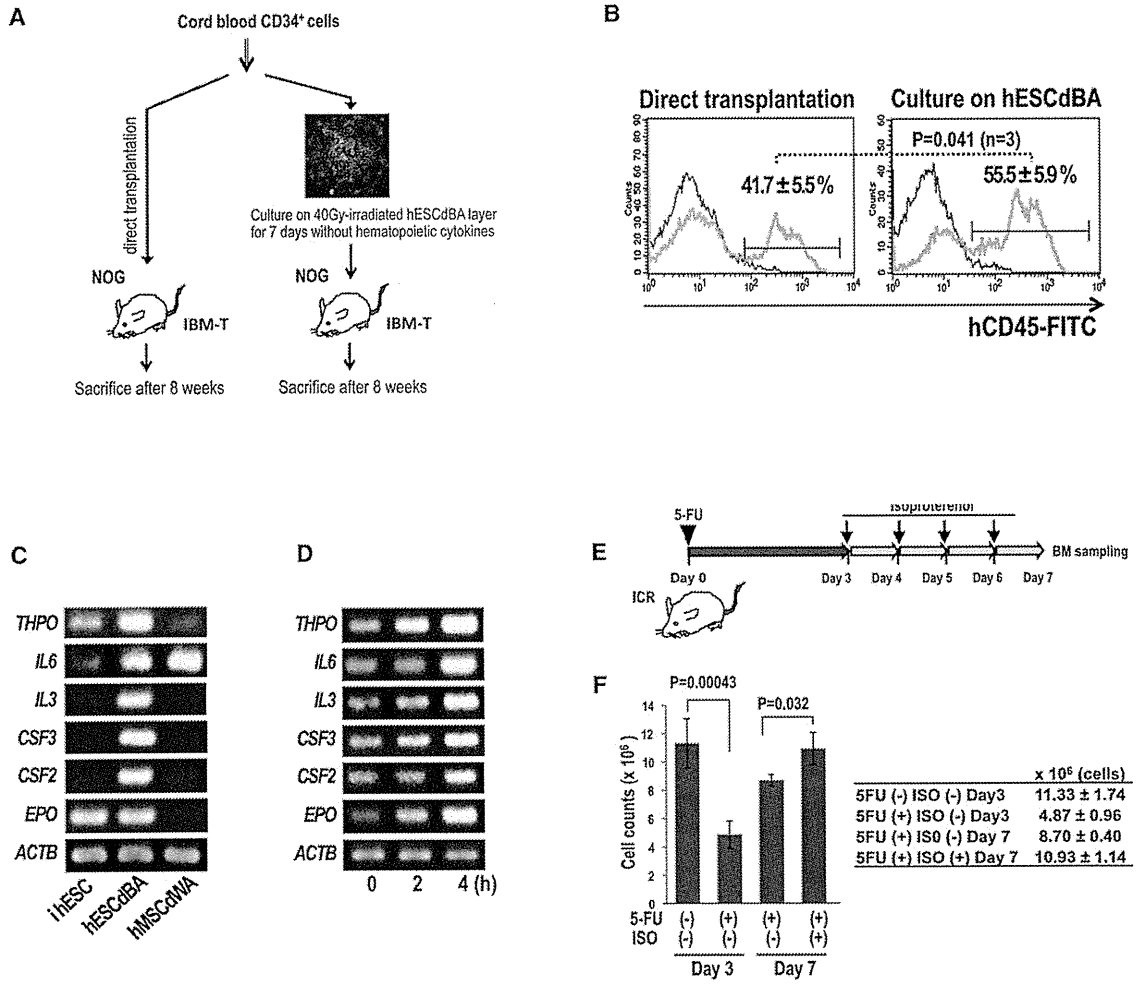

Figure 6. Hematopoietic Stromal Assays

(A) Schematic presentation of the assay.

(B) After 8 weeks from transplantation, cells were collected from the spleen and subjected to flow cytometry. hCD45-positive percentages were calculated. Similar results were obtained at 6 and 12 weeks after transplantation (data not shown). The error bars represent average ± SD (n = 3).

(C and D) Various hematopoietin expression was examined by RT-PCR in immature hESCs (ihESCs), hESCdBAs, and hMSCdWAs (C). Hematopoietin expression in hESCdBAs after isoproterenol treatments was examined over time by RT-PCR (D).

(E and F) 5-FU treatment assay. Experimental procedure (E) and the results of BM-enucleated cell counts (F) were shown. The error bars represent average ± SD (n = 3).

hESC/hiPSC-derived spheres were further cultured on gelatin-coated 6-well plates using the above-described serum-free medium supplemented with the hematopoietic cytokine cocktail II (5 ng/ml IGF-II, 10 ng/ml BMP7, 5 ng/ml VEGFA, 20 ng/ml KITLG, 2.5 ng/ml FLT3LG, 2.5 ng/ml IL-6) for several days.

Protein Expression Analyses

Immunostaining was performed using a goat polyclonal anti-human UCP1 antibody (sc-6528, Santa Cruz Biotechnology, Inc.) or a rabbit polyclonal anti-human SOD2 antibody LS-C39331, LifeSpan BioSciences Inc., Seattle, WA) as described previously (Nakahara et al., 2009). Western blotting was performed using a rabbit polyclonal UCP1 (Ab10983) (Abcam plc., Cambridge, UK) as described previously (Nakahara et al., 2009).

Gene Expression Analyses

RT-PCR was performed using primers described in Supplemental Information. Quantitative RT-PCR (qPCR) was performed by applying SYBR Green qPCR method using primers purchased from SuperArray (QIAGEN Science, Maryland, USA) as described in the Supplemental Experimental Procedures. The results were normalized by *GAPDH*.

Electron Microscopic Examinations

Cells were fixed by 2.5% glutaraldehyde. Postfixation by 2% osmium tetroxide, along with sample embedding into resin and slicing, was performed by Bio Medical Laboratories Co. Ltd. (Tokyo, Japan) (Saeki et al., 2000).

Inhibitor Analyses

BA differentiation was performed by adding the following inhibitors to the differentiation medium: 10 μM p38 MAP kinase inhibitor (Cat 506126) (Calbiochem Co., Darmstadt, Germany), 50 μM MEK1 inhibitor (PD 98059) (Calbiochem Co.), 10 μM BMPR1a inhibitor (Dorsomorphin Dihydrochloride, Cat 047-31801) (WAKO Pure Chemical Industries, Osaka, Japan), and 10 μM Akt inhibitor IV (Cat 124011) (Calbiochem Co.).

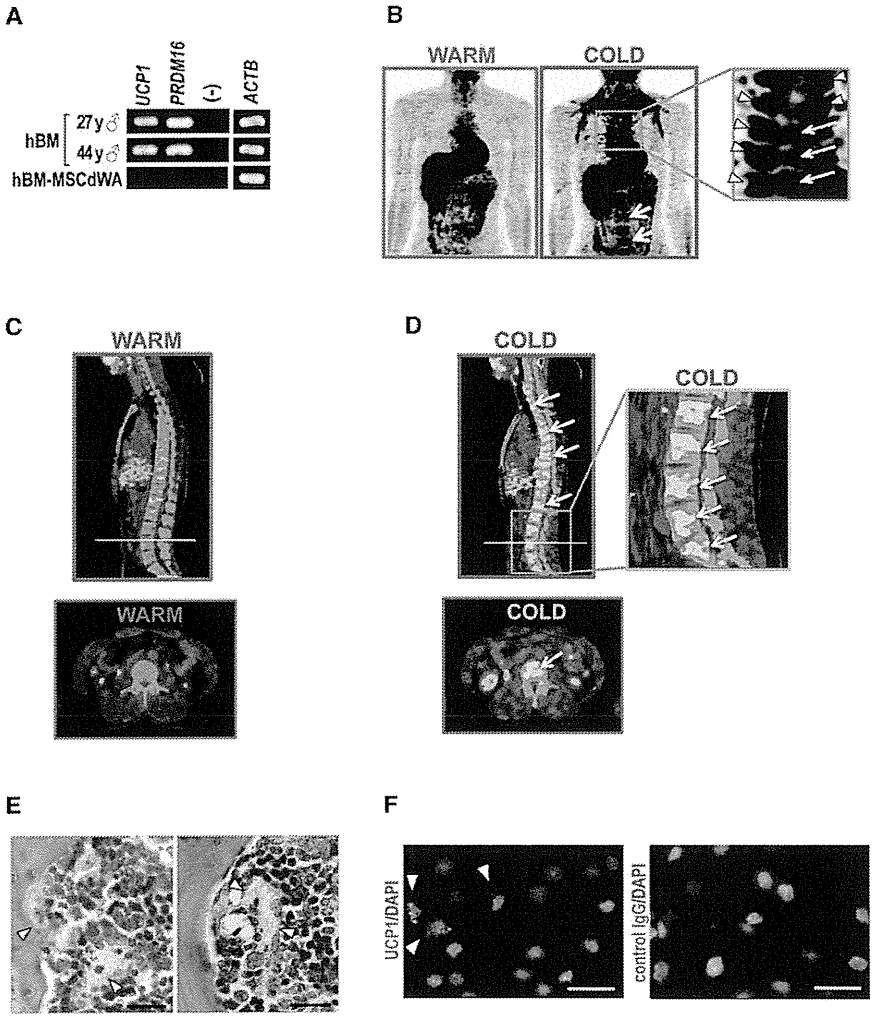

Figure 7. Examinations on BM-BAT

(A) Expression of *PRDM16* and *UCP1* in BM RNA samples of 27-year-old and 41-year-old males and human BM-derived hMSCdWA (hBM-MCdWA).

(B) ^{18}F-FDG-PET/CT. Typical results of the frontal images under warm and cold conditions were shown. Arrows indicate ^{18}F-FDG uptake into vertebrae per se, and arrowheads indicate ^{18}F-FDG uptake into classical paravertebral BA.

(C and D) Shown are sagittal and axial section images of ^{18}F-FDG-PET/CT under warm (C) and cold conditions (D). Arrows indicate the ^{18}F-FDG uptake into vertebral BM.

(E and F) Thoracic vertebra of 3-week-old ICR mice was subjected to HE staining (E) or UCP1 immunostaining (FF). Arrowheads indicate the existence of BA.

were measured by Accutrend Plus (F. Hoffmann-La Roche, Ltd., Basel, Switzerland). For oral fat tolerance tests, ICR mice were subcutaneously transplanted with immature hPSC or hPSCdBA and kept abstained from feed. After 16 hr, isoproterenol (15 μmol/kg) was administrated. After another 2 hr, 200 μl of olive oil was orally administrated, and blood TG levels were measured every 2 hr.

Assessment of Glucose Metabolism

The 1 × 10^6 of hESCdBA or hMSCdWA was transplanted to 6- or 10-week-old male ICR mice, which were kept abstained from feed. After 16 hr, isoproterenol (30 μmol/kg) was administrated. After another 4 hr, 2 g/kg of glucose (041-00595, Wako Pure Chemical Industries, Ltd., Osaka, Japan) was orally administrated. Blood sample were taken after 0, 15, 30, and 60 min. Blood glucose concentrations were measured by Accutrend Plus, and plasma insulin concentrations were measured by mouse insulin ELISA kit (Morinaga Institute of Biological Science, Inc., Yokohama, Japan).

Oxygen Consumption Analyses

The adherent culture step of BA differentiation was performed on special 96-well plates (Seahorse Bioscience Inc., Billerica, MA) precoated by 0.1% gelatin by seeding 30 spheres per well. Oxygen consumption was analyzed by Extracellular Flux Analyzer XF96 (Seahorse Bioscience Inc.) according to the manufacturer's guidance.

Calorigenic Analyses

The 1 × 10^6 of hPSCdBA or immature hPSCs were suspended in 100 μl saline and subcutaneously transplanted into 5-week-old male ICR mice After 24 hr, 30 μmol/kg of isoproterenol (12760, Sigma Chemical Co.) was administrated from the tail vein. After another 4 hr, mice were anesthetized, and dermal temperature was measured by Thermo GEAR G120/G100 (NEC Avio Infrared Technologies Co., Ltd, Tokyo, Japan). All animal care procedures involved in calorigenic analyses, assessment of lipid and metabolism, and hematopoietic stromal assays were approved by the Animal Care and Use Committee of the Research Institute, National Center for Global Health and Medicine (NCGM), and complied with the procedures of the Guide for the Care and Use of Laboratory Animals of NCGM.

Assessment of Lipid Metabolism

Six-week-old male CR mice were subcutaneously transplanted with 1 × 10^6 of immature hESC, hESCdBA, or hMC-derived WA suspended in 100 μl saline and kept abstained from feed. After 16 hr, isoproterenol (30 μmol/kg) was administrated. After another 2 hr, blood samples were taken, and TG concentrations

Hematopoietic Stromal Assays

The human cord blood CD34$^+$ cells were cultured on hPSCdBA layers without recombinant cytokines in RPMI1640 medium supplemented with 10% fetal calf serum. Floating cells were collected after 7 days, and 2 × 10^5 cells were transplanted into tibial bone marrow of NOG mice. After 6, 8, and 12 weeks, cells were collected from contralateral femoral bone marrow and spleen and subjected to cytometry using an anti-human CD45-FITC (clone J33) (Beckman Coulter Inc.) and anti-human CD33-PE antibody (clone WM53) (BD Biosciences, San Jose, CA). For control, cord blood CD34$^+$ cells were directly transplanted without coculture. For myelosuppression recovery assays, 100 mg/kg of 5-FU was intraperitoneally administrated. From day 3 to day 6, 30 μmol/kg of isoproterenol was administrated from tail vein. At day 7, bone marrow cells were collected from femoral bones and analyzed.

^{18}F-FDG-PET/CT Examinations

After careful instruction regarding the study and informed consent to participants, PET/CT examinations of healthy young volunteers (24.8 ± 5.8 years of age, n = 20) were performed. The protocol was approved by the institutional review boards of Tenshi College. Standardized uptake value (SUV) was measured by an expert as described in the Supplemental Experimental Procedures. Data are reported as means ± SEM. Statistics analyses were performed using SPSS software, version 18 (International Business Machines

Corp, New York), as described in the Supplemental Experimental Procedures. P values are considered to be statistically significant if <0.05.

SUPPLEMENTAL INFORMATION

Supplemental Information includes seven figures, Supplemental Experimental Procedures, and Supplemental References and can be found with this article online at http://dx.doi.org/10.1016/j.cmet.2012.08.001.

ACKNOWLEDGMENTS

This work was supported by Grant-in-Aid from Ministry of Health, Labour and Welfare of Japan (KHD1017) and by Japan Science and Technology Agency (AS 2321379G). We thank Mr. Kameya at LSI Sapporo Clinic for technical assistance for PET-CT examinations and Mr. Obara at LSI Sapporo Clinic for general assistance.

Received: March 17, 2012
Revised: June 30, 2012
Accepted: August 1, 2012
Published online: September 4, 2012

REFERENCES

Ahfeldt, T., Schinzel, R.T., Lee, Y.K., Hendrickson, D., Kaplan, A., Lum, D.H., Camahort, R., Xia, F., Shay, J., Rhee, E.P., et al. (2012). Programming human pluripotent stem cells into white and brown adipocytes. Nat. Cell Biol. *14*, 209–219.

Arai, F., and Suda, T. (2007). Maintenance of quiescent hematopoietic stem cells in the osteoblastic niche. Ann. N Y Acad. Sci. *1106*, 41–53.

Asano, A., Morimatsu, M., Nikami, H., Yoshida, T., and Saito, M. (1997). Adrenergic activation of vascular endothelial growth factor mRNA expression in rat brown adipose tissue: implication in cold-induced angiogenesis. Biochem. J. *328*, 179–183.

Bartelt, A., Bruns, O.T., Reimer, R., Hohenberg, H., Ittrich, H., Peldschus, K., Kaul, M.G., Tromsdorf, U.I., Weller, H., Waurisch, C., et al. (2011). Brown adipose tissue activity controls triglyceride clearance. Nat. Med. *17*, 200–205.

Braun, T., and Arnold, H.H. (1996). Myf-5 and myoD genes are activated in distinct mesenchymal stem cells and determine different skeletal muscle cell lineages. EMBO J. *15*, 310–318.

Calo, E., Quintero-Estades, J.A., Danielian, P.S., Nedelcu, S., Berman, S.D., and Lees, J.A. (2010). Rb regulates fate choice and lineage commitment in vivo. Nature *466*, 1110–1114.

Cossu, G., Kelly, R., Tajbakhsh, S., Di Donna, S., Vivarelli, E., and Buckingham, M. (1996). Activation of different myogenic pathways: myf-5 is induced by the neural tube and MyoD by the dorsal ectoderm in mouse paraxial mesoderm. Development *122*, 429–437.

Crisan, M., Yap, S., Casteilla, L., Chen, C.W., Corselli, M., Park, T.S., Andriolo, G., Sun, B., Zheng, B., Zhang, L., et al. (2008). A perivascular origin for mesenchymal stem cells in multiple human organs. Cell Stem Cell *3*, 301–313.

Cypess, A.M., Lehman, S., Williams, G., Tal, I., Rodman, D., Goldfine, A.B., Kuo, F.C., Palmer, E.L., Tseng, Y.H., Doria, A., et al. (2009). Identification and importance of brown adipose tissue in adult humans. N. Engl. J. Med. *360*, 1509–1517.

Dexter, T.M., Allen, T.D., and Lajtha, L.G. (1977). Conditions controlling the proliferation of haemopoietic stem cells in vitro. J. Cell. Physiol. *91*, 335–344.

Elabd, C., Chiellini, C., Carmona, M., Galitzky, J., Cochet, O., Petersen, R., Pénicaud, L., Kristiansen, K., Bouloumié, A., Casteilla, L., et al. (2009). Human multipotent adipose-derived stem cells differentiate into functional brown adipocytes. Stem Cells *27*, 2753–2760.

Enerbäck, S., Jacobsson, A., Simpson, E.M., Guerra, C., Yamashita, H., Harper, M.E., and Kozak, L.P. (1997). Mice lacking mitochondrial uncoupling protein are cold-sensitive but not obese. Nature *387*, 90–94.

Feldmann, H.M., Golozoubova, V., Cannon, B., and Nedergaard, J. (2009). UCP1 ablation induces obesity and abolishes diet-induced thermogenesis in mice exempt from thermal stress by living at thermoneutrality. Cell Metab. *9*, 203–209.

Gimble, J.M., Dorheim, M.A., Cheng, Q., Medina, K., Wang, C.S., Jones, R., Koren, E., Pietrangeli, C., and Kincade, P.W. (1990). Adipogenesis in a murine bone marrow stromal cell line capable of supporting B lineage lymphocyte growth and proliferation: biochemical and molecular characterization. Eur. J. Immunol. *20*, 379–387.

Gimble, J.M., Youkhana, K., Hua, X., Bass, H., Medina, K., Sullivan, M., Greenberger, J., and Wang, C.S. (1992). Adipogenesis in a myeloid supporting bone marrow stromal cell line. J. Cell. Biochem. *50*, 73–82.

Gupta, R.K., Mepani, R.J., Kleiner, S., Lo, J.C., Khandekar, M.J., Cohen, P., Frontini, A., Bhowmick, D.C., Ye, L., Cinti, S., et al. (2012). Zfp423 expression identifies committed preadipocytes and localizes to adipose endothelial and perivascular cells. Cell Metab. *15*, 230–239.

Hiroyama, T., Miharada, K., Aoki, N., Fujioka, T., Sudo, K., Danjo, I., Nagasawa, T., and Nakamura, Y. (2006). Long-lasting in vitro hematopoiesis derived from primate embryonic stem cells. Exp. Hematol. *34*, 760–769.

Hofer, M., Pospísil, M., Znojil, V., Holá, J., Vacek, A., and Streitová, D. (2007). Adenosine A(3) receptor agonist acts as a homeostatic regulator of bone marrow hematopoiesis. Biomed. Pharmacother. *61*, 356–359.

Ito, M., Hiramatsu, H., Kobayashi, K., Suzue, K., Kawahata, M., Hioki, K., Ueyama, Y., Koyanagi, Y., Sugamura, K., Tsuji, K., et al. (2002). NOD/SCID/gamma(c)(null) mouse: an excellent recipient mouse model for engraftment of human cells. Blood *100*, 3175–3182.

Jacene, H.A., Cohade, C.C., Zhang, Z., and Wahl, R.L. (2011). The relationship between patients' serum glucose levels and metabolically active brown adipose tissue detected by PET/CT. Mol. Imaging Biol. *13*, 1278–1283.

Jackson, D.M., Hambly, C., Trayhurn, P., and Speakman, J.R. (2001). Can non-shivering thermogenesis in brown adipose tissue following NA injection be quantified by changes in overlying surface temperatures using infrared thermography? J. Therm. Biol. *26*, 85–93.

Kiel, M.J., and Morrison, S.J. (2006). Maintaining hematopoietic stem cells in the vascular niche. Immunity *25*, 862–864.

Kontani, Y., Wang, Y., Kimura, K., Inokuma, K.I., Saito, M., Suzuki-Miura, T., Wang, Z., Sato, Y., Mori, N., and Yamashita, H. (2005). UCP1 deficiency increases susceptibility to diet-induced obesity with age. Aging Cell *4*, 147–155.

Krings, A., Rahman, S., Huang, S., Lu, Y., Czernik, P.J., and Lecka-Czernik, B. (2012). Bone marrow fat has brown adipose tissue characteristics, which are attenuated with aging and diabetes. Bone *50*, 546–552.

Laharrague, P., Fontanilles, A.M., Tkaczuk, J., Corberand, J.X., Pénicaud, L., and Casteilla, L. (2000). Inflammatory/haematopoietic cytokine production by human bone marrow adipocytes. Eur. Cytokine Netw. *11*, 634–639.

Motyl, K.J., and Rosen, C.J. (2011). Temperatures rising: brown fat and bone. Discov. Med. *11*, 179–185.

Nagasawa, T. (2007). The chemokine CXCL12 and regulation of HSC and B lymphocyte development in the bone marrow niche. Adv. Exp. Med. Biol. *602*, 69–75.

Nakahara, M., Nakamura, N., Matsuyama, S., Yogiashi, Y., Yasuda, K., Kondo, Y., Yuo, A., and Saeki, K. (2009). High-efficiency production of subculturable vascular endothelial cells from feeder-free human embryonic stem cells without cell-sorting technique. Cloning Stem Cells *11*, 509–522.

Naveiras, O., Nardi, V., Wenzel, P.L., Hauschka, P.V., Fahey, F., and Daley, G.Q. (2009). Bone-marrow adipocytes as negative regulators of the haematopoietic microenvironment. Nature *460*, 259–263.

Ookura, N., Fujimori, Y., Nishioka, K., Kai, S., Hara, H., and Ogawa, H. (2007). Adipocyte differentiation of human marrow mesenchymal stem cells reduces the supporting capacity for hematopoietic progenitors but not for severe combined immunodeficiency repopulating cells. Int. J. Mol. Med. *19*, 387–392.

Osafune, K., Caron, L., Borowiak, M., Martinez, R.J., Fitz-Gerald, C.S., Sato, Y., Cowan, C.A., Chien, K.R., and Melton, D.A. (2008). Marked differences in differentiation propensity among human embryonic stem cell lines. Nat. Biotechnol. *26*, 313–315.

Ouellet, V., Routhier-Labadie, A., Bellemare, W., Lakhal-Chaieb, L., Turcotte, E., Carpentier, A.C., and Richard, D. (2011). Outdoor temperature, age, sex, body mass index, and diabetic status determine the prevalence, mass, and glucose-uptake activity of 18F-FDG-detected BAT in humans. J. Clin. Endocrinol. Metab. *96*, 192–199.

Petrovic, N., Walden, T.B., Shabalina, I.G., Timmons, J.A., Cannon, B., and Nedergaard, J. (2010). Chronic peroxisome proliferator-activated receptor gamma (PPARgamma) activation of epididymally derived white adipocyte cultures reveals a population of thermogenically competent, UCP1-containing adipocytes molecularly distinct from classic brown adipocytes. J. Biol. Chem. *285*, 7153–7164.

Reznikoff, C.A., Brankow, D.W., and Heidelberger, C. (1973). Establishment and characterization of a cloned line of C3H mouse embryo cells sensitive to postconfluence inhibition of division. Cancer Res. *33*, 3231–3238.

Saeki, K., Yuo, A., Okuma, E., Yazaki, Y., Susin, S.A., Kroemer, G., and Takaku, F. (2000). Bcl-2 down-regulation causes autophagy in a caspase-independent manner in human leukemic HL60 cells. Cell Death Differ. *7*, 1263–1269.

Saito, M., Okamatsu-Ogura, Y., Matsushita, M., Watanabe, K., Yoneshiro, T., Nio-Kobayashi, J., Iwanaga, T., Miyagawa, M., Kameya, T., Nakada, K., et al. (2009). High incidence of metabolically active brown adipose tissue in healthy adult humans: effects of cold exposure and adiposity. Diabetes *58*, 1526–1531.

Sakurai, H., Era, T., Jakt, L.M., Okada, M., Nakai, S., Nishikawa, S., and Nishikawa, S. (2006). In vitro modeling of paraxial and lateral mesoderm differentiation reveals early reversibility. Stem Cells *24*, 575–586.

Seale, P., Kajimura, S., Yang, W., Chin, S., Rohas, L.M., Uldry, M., Tavernier, G., Langin, D., and Spiegelman, B.M. (2007). Transcriptional control of brown fat determination by PRDM16. Cell Metab. *6*, 38–54.

Seale, P., Bjork, B., Yang, W., Kajimura, S., Chin, S., Kuang, S., Scimè, A., Devarakonda, S., Conroe, H.M., Erdjument-Bromage, H., et al. (2008). PRDM16 controls a brown fat/skeletal muscle switch. Nature *454*, 961–967.

Sellayah, D., Bharaj, P., and Sikder, D. (2011). Orexin is required for brown adipose tissue development, differentiation, and function. Cell Metab. *14*, 478–490.

Suemori, H., Yasuchika, K., Hasegawa, K., Fujioka, T., Tsuneyoshi, N., and Nakatsuji, N. (2006). Efficient establishment of human embryonic stem cell lines and long-term maintenance with stable karyotype by enzymatic bulk passage. Biochem. Biophys. Res. Commun. *345*, 926–932.

Sun, L., Xie, H., Mori, M.A., Alexander, R., Yuan, B., Hattangadi, S.M., Liu, Q., Kahn, C.R., and Lodish, H.F. (2011). Mir193b-365 is essential for brown fat differentiation. Nat. Cell Biol. *13*, 958–965.

Takayama, N., Nishikii, H., Usui, J., Tsukui, H., Sawaguchi, A., Hiroyama, T., Eto, K., and Nakauchi, H. (2008). Generation of functional platelets from human embryonic stem cells in vitro via ES-sacs, VEGF-promoted structures that concentrate hematopoietic progenitors. Blood *111*, 5298–5306.

Tanaka, Y., and Inoue, T. (1976). Fatty marrow in the vertebrae. A parameter for hematopoietic activity in the aged. J. Gerontol. *31*, 527–532.

Thorns, C., Schardt, C., Katenkamp, D., Kähler, C., Merz, H., and Feller, A.C. (2008). Hibernoma-like brown fat in the bone marrow: report of a unique case. Virchows Arch. *452*, 343–345.

Timmons, J.A., Wennmalm, K., Larsson, O., Walden, T.B., Lassmann, T., Petrovic, N., Hamilton, D.L., Gimeno, R.E., Wahlestedt, C., Baar, K., et al. (2007). Myogenic gene expression signature establishes that brown and white adipocytes originate from distinct cell lineages. Proc. Natl. Acad. Sci. USA *104*, 4401–4406.

Tonello, C., Giordano, A., Cozzi, V., Cinti, S., Stock, M.J., Carruba, M.O., and Nisoli, E. (1999). Role of sympathetic activity in controlling the expression of vascular endothelial growth factor in brown fat cells of lean and genetically obese rats. FEBS Lett. *442*, 167–172.

Tran, K.V., Gealekman, O., Frontini, A., Zingaretti, M.C., Morroni, M., Giordano, A., Smorlesi, A., Perugini, J., De Matteis, R., Sbarbati, A., et al. (2012). The vascular endothelium of the adipose tissue gives rise to both white and brown fat cells. Cell Metab. *15*, 222–229.

Tseng, Y.H., Kokkotou, E., Schulz, T.J., Huang, T.L., Winnay, J.N., Taniguchi, C.M., Tran, T.T., Suzuki, R., Espinoza, D.O., Yamamoto, Y., et al. (2008). New role of bone morphogenetic protein 7 in brown adipogenesis and energy expenditure. Nature *454*, 1000–1004.

van Marken Lichtenbelt, W.D., Vanhommerig, J.W., Smulders, N.M., Drossaerts, J.M., Kemerink, G.J., Bouvy, N.D., Schrauwen, P., and Teule, G.J. (2009). Cold-activated brown adipose tissue in healthy men. N. Engl. J. Med. *360*, 1500–1508.

Virtanen, K.A., Lidell, M.E., Orava, J., Heglind, M., Westergren, R., Niemi, T., Taittonen, M., Laine, J., Savisto, N.J., Enerbäck, S., and Nuutila, P. (2009). Functional brown adipose tissue in healthy adults. N. Engl. J. Med. *360*, 1518–1525.

Yoneshiro, T., Aita, S., Matsushita, M., Okamatsu-Ogura, Y., Kameya, T., Kawai, Y., Miyagawa, M., Tsujisaki, M., and Saito, M. (2011). Age-related decrease in cold-activated brown adipose tissue and accumulation of body fat in healthy humans. Obesity (Silver Spring) *19*, 1755–1760.

CHEMICAL REVIEWS

Review

pubs.acs.org/CR

Biomimetic Cell Culture Proteins as Extracellular Matrices for Stem Cell Differentiation

Akon Higuchi,*[,†,‡,§] Qing-Dong Ling,[§,∥] Shih-Tien Hsu,[⊥] and Akihiro Umezawa[‡]

[†]Department of Chemical and Materials Engineering, National Central University, Jhongli, Taoyuan, 32001 Taiwan

[‡]Department of Reproductive Biology, National Research Institute for Child Health and Development, 2-10-1 Okura, Setagaya-ku, Tokyo 157-8535, Japan

[§]Cathay Medical Research Institute, Cathay General Hospital, No. 32, Ln 160, Jian-Cheng Road, Hsi-Chi City, Taipei, 221 Taiwan

[∥]Institute of Systems Biology and Bioinformatics, National Central University, No. 300, Jhongda RD., Jhongli, Taoyuan, 32001 Taiwan

[⊥]Taiwan Landseed Hospital, 77 Kuangtai Road, Pingjen City, Tao-Yuan County, 32405 Taiwan

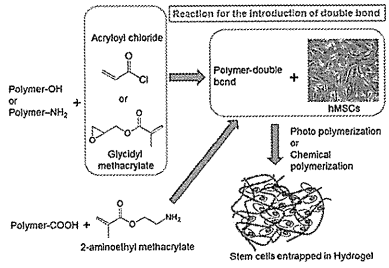

CONTENTS

1. INTRODUCTION

Each year, millions of people suffer loss or damage to organs and tissues due to accidents, birth defects, and disease. Stem cells are an attractive prospect for tissue engineering and regenerative medicine because of their unique biological properties. Embryonic stem cells (ESCs) derived from

Received: January 14, 2012
Published: May 23, 2012

   dx.doi.org/10.1021/cr3000169 | Chem. Rev. 2012, 112, 4507–4540

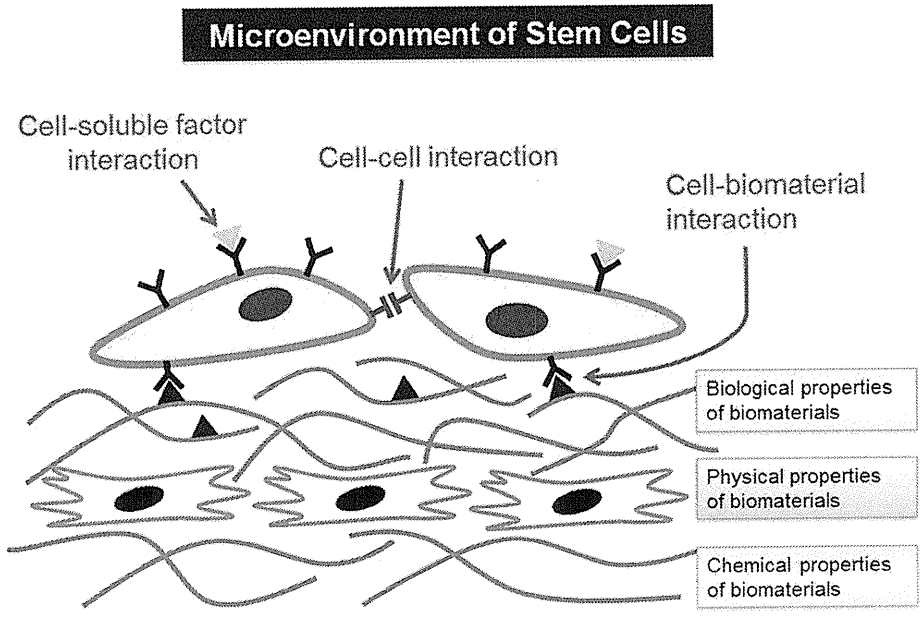

Figure 1. Schematic representation of the microenvironment and niches of stem cells and their regulation by the following factors: (a) soluble factors, such as growth factors or cytokines, nutrients, and bioactive molecules; (b) cell–cell interactions; (c) cell–biomaterial interactions. Biological, physical, and chemical properties of biomaterials also regulate stem cell fate.

preimplantation embryos have the potential to differentiate into any cell type derived from the three germ layers—the ectoderm (epidermal tissues and nerves), mesoderm (muscle, bone, and blood), and endoderm (liver, pancreas, gastrointestinal tract, and lungs).[1] The basis of pluripotency lies in conserved regulatory networks composed of numerous transcription factors and multiple signaling cascades. Together, these regulatory networks maintain human ESCs (hESCs) in a pluripotent and undifferentiated state, and alterations in the stoichiometry of these signals promote differentiation. hESCs have been shown to generate multipotent stem and progenitor cells in vitro and are capable of differentiating into a limited number of cell fates, and thus they have great potential for use in transplantation of cells and tissues into patients.[2]

Although hESCs are promising donor sources for cell transplantation therapies,[1] they face immune rejection after transplantation. Furthermore, ethical issues regarding human embryos hinder their widespread usage. These concerns can be circumvented if pluripotent stem cells can be derived directly from patients' own somatic cells.[3] Recently, pluripotent stem cells similar to ESCs, known as induced pluripotent stem cells (iPSC's), were derived from adult somatic cells by inducing a "forced" expression of certain pluripotent (stem cell) genes[4−6] such as Oct3/4, Sox2, (c-myc), and klf-4, or certain miRNAs[7] or proteins (piPS).[8] iPSC's are believed to be similar to ESCs in many respects, including the expression of certain stem cell genes and proteins, chromatin methylation patterns, doubling time, embryoid body formation, teratoma formation, viable chimera formation, pluripotency, and differentiability.

The pluripotent nature of iPSC's opens many avenues for potential stem cell-based regenerative therapies and for development of drug-discovery platforms.[9,10] The nearest-term therapeutic uses of iPSC's may exist in the transplantation of differentiated nerve cells or β-cells for treatment of Parkinson's Disease and diabetes, respectively, which arise from disorders of single cell types. However, there are several barriers to the clinical application of iPSC's, such as the use of viral vectors, cultivation using xeno-derived materials [e.g., mouse embryonic fibroblasts (MEFs)], and the extremely low efficiency of iPSC generation.[11]

Stem cells have also been isolated from a variety of somatic tissues, including hematopoietic stem cells (HSCs) derived from umbilical cord blood and mesenchymal stem cells (MSCs) derived from bone marrow, umbilical cord blood, umbilical cord, dental pulp, and tissues such as fat. There have been no reports to date of MSCs or fetal stem cells differentiating into tumors, unlike ESCs and iPSC's. Consequently, HSCs, MSCs, and fetal stem cells are the most promising sources of cells for tissue engineering and cell therapies. Currently, MSCs are thought to be the most widely available autologous source of stem cells for practical and clinical applications. Fetal stem cells derived from amniotic fluid are pluripotent cells capable of differentiating into multiple lineages, including cell types of the three embryonic germ layers. Bone marrow MSCs, adipose-derived stem cells (ADSCs), and amniotic fluid stem cells may be more suitable sources of stem cells in regenerative medicine and tissue engineering than ESCs and iPSC's because of ethical concerns regarding their use and concerns about xenogenic contamination arising from the use of mouse embryonic fibroblasts (MEFs) as a feeder layer for ESC and iPSC culture.[11]

Stem cell characteristics, such as proper differentiation and maintenance of pluripotency, are regulated not only by the stem cells themselves but also by the microenvironment. Therefore, mimicking stem cell microenvironments and niches using biopolymers will facilitate the production of large numbers of stem cells and specifically differentiated cells needed for in vitro regenerative medicine. Several factors in the microenvironment and niches of stem cells influence their fate: (i) soluble factors, such as growth factors or cytokines, nutrients, and bioactive molecules; (ii) cell–cell interactions; (iii) cell–biomacromolecule (or biomaterial) interactions; and (iv) physical factors, such as the rigidity of the environment (Figure 1). Some excellent review articles addressing the

dx.doi.org/10.1021/cr3000169 | Chem. Rev. 2012, 112, 4507–4540

engineering of stem cell microenvironments and niches using natural and synthetic biopolymers are listed in Table 1.[11−22]

Table 1. Key Review and Articles Dealing with Biopolymers for Culture and Differentiation of Stem and Progenitor Cells

author	contents	ref (year)
Lee and Mooney	hydrogels for tissue engineering	12 (2001)
Little et al.	biomaterials for neural stem cell microenvironments	13 (2008)
Higuchi et al.	polymeric materials for ex vivo expansion of HSCs	16 (2009)
Mei et al.	combinatorial development of biomaterials for clonal growth of human pluripotent stem cells	17 (2010)
Melkoumian et al.	synthetic peptide-acrylate surfaces for long-term self-renewal of hESCs	18 (2010)
G. J. Delcroix et al.	adult cell therapy for brain neuronal damages and the role of tissue engineering	22 (2010)
Higuchi et al.	biomaterials for the feeder-free culture of hESCs and human iPSC's	11 (2011)
Balakrishnam and Banerjee	biopolymer-based hydrogels for cartilage tissue engineering	14 (2011)
Kim et al.	design of artificial extracellular matrices for tissue engineering	15 (2011)
Engler et al.	matrix elasticity directs stem cell lineage	19 (2006)
Gilbert et al.	substrate elasticity regulates skeletal muscle stem cell self-renewal	20 (2010)
Huebsch et al.	harnessing traction-mediated manipulation of the cell/matrix interface to control stem-cell fate	21 (2010)

These articles focus on biopolymers employed for maintenance of pluripotency of hESCs, iPSC's, or hematopoietic stem cells (HSCs),[16−18] and for specific differentiation lineages such as chondrocytes (cartilage), muscle cells, and neural cells.[13,14,20] There have been no review articles specifically describing extracellular matrix (ECM) scaffolds (ECM in 3D) or ECM-immobilized dish coatings (ECM in 2D) that guide stem cell fates and differentiation. Therefore, this review focuses on the chemical, physical, and biological characteristics of natural biopolymers, especially ECM proteins, which are the major functional biopolymers, and deals with the ability of these biopolymers to guide differentiation of MSCs into osteogenic, chondrogenic, adipogenic, cardiomyogenic, and neural cell lineages.

2. CELL SOURCES AND ANALYSIS OF DIFFERENTIATION LINEAGES OF MSCS

2.1. Cell Sources

Human MSCs (hMSCs), including fetal stem cells, are one of the most widely available autologous sources of stem cells for clinical applications. hMSCs can be obtained from bone marrow,[23,24] adipose tissue,[25,26] dental pulp,[27] and urine,[28] among other sources. Fetal stem cells can be obtained from amniotic fluid,[29−31] umbilical cord,[32−34] menstrual blood,[35,36] umbilical cord blood,[25,34,37] and placenta.[38,39] hMSCs derived from bone marrow and fat are primarily used for biomaterials research on stem cell culture and differentiation because bone marrow MSCs and ADSCs are easily accessible and can be obtained in large quantities. Bone marrow MSCs (BMSCs) are now commercially available from several companies. Stem cell research is facilitated with these stem cell sources because it is not necessary to obtain permission from ethics committees of the Institutional Review Board (IRB) for use of commercially available MSCs. Otherwise, informed consent from donors and permission from the IRB must be obtained.

2.2. Analysis of Differentiation Lineages

MSCs are multipotent stem cells that can be differentiated into various mesodermal lineages, including osteoblasts, chondrocytes (cartilages), adipocytes, myocytes, and cardiomyocytes.[19,40,41] MSCs are also reported to be able to differentiate into ectodermal lineages (e.g., neuron, oligodendrocyte, astrocyte, neural stem cells, and dopamine-secreting cells)[22,42−45] and endodermal lineages (hepatocytes and β-cells),[31,46−52] although with lower probability than mesoderm lineages. Table 2 summarizes methods for characterizing specific differentiated cells from MSCs.[11,34,46,48,51−87]

MSCs differentiate into an osteogenic phenotype in vitro when supplements such as ascorbic acid, β-glycerophosphate, dexamethasone, and/or bone morphogenic protein 2 (BMP-2) are added to the culture medium. Figure 2 shows the expression of several genes and proteins, as well as mineral deposition, by MSCs upon osteogenic differentiation. Runt-related transcription factor 2 (Runx2, also known as Cbfa1, Pebp2αA, and AML3) is a master regulator of osteogenic gene expression and osteoblast differentiation, and it is an early marker of osteogenesis.[88−90] Runx2 activity is stimulated by mitogen-activated protein kinase (MAPK) signaling and is negatively regulated by thrombin-like enzyme 2 (TLE2). Alkaline phosphatase (ALP) activity is an early osteogenic marker, and osteopontin and osteocalcin are late osteogenic markers.[88] Mineral deposition is generated in the late stage of osteogenic differentiation and is detected by Alizarin Red staining (calcium deposition) and von Kossa staining (calcium phosphate deposition).[57,60,62]

MSCs commit to a chondrogenic phenotype when supplied with transforming growth factor-β1 (TGF-β1). Chondrogenic differentiation of MSCs is typically determined by immunostaining for specific proteins, such as collagen type II and Sox9, dye labeling of glycosamino glycans, and evaluation of expression of chondrogenic proteins or transcription factors (such as collagen type II and type X, cartilage oligomeric protein, aggrecan, and Sox9) (Table 2).[63,64,67,70,91] Sulfated glycosaminoglycans (sGAG's) are visualized by staining with Alcian blue.[91] Accumulation of sulfated proteoglycans are also visualized by Safranin O staining.[72]

Only a few groups have investigated adipogenic differentiation of MSCs cultured on natural and artificial biomaterials[53,62,70,74,75,92] because adipose tissue is in less demand in clinical usage than osteoblasts and cartilage cells. Adipogenic differentiation is also analyzed by immunostaining for specific proteins (vimentin), dye staining of oil droplets, and measuring expression of transcription factors or other marker proteins, such as peroxisome proliferator-activated receptorγ [PPARγ] and adipocyte Protein 2 (aP-2).[53,61,62,74,75,92] aP-2 is a carrier protein for fatty acids that is primarily expressed in adipocytes.[93] Preadipocytes and mature adipocytes contain multiple or single lipids in cell bodies, respectively. Therefore, Oil Red O or Nile red staining of preadipocytes and mature adipocytes is frequently used for the detection of lipids.

Neural differentiation of MSCs is primarily analyzed by observing characteristic morphologies of neurons, astrocytes, oligodendrocytes, and microglia. Neuronal progenitor cells and early-stage neurons are also identified by Sox1, Sox2, and CD133 gene expression and by nestin and β-tubulin-III

dx.doi.org/10.1021/cr3000169 | Chem. Rev. 2012, 112, 4507−4540

Table 2. Characterization of Differentiation of MSCs into Specific Lineages [Osteoblasts and Chondrocyte (Cartilages)]

differentiation lineage	characterization	specification	ref (example)
1. Osteoblast	morphology	spread shape tends to differentiate into osteoblasts, bonelike nodule formation	53−55
	protein level (immunostaining)	**collagen I**, osteocalcin, osteonectin	56, 57
	surface marker analysis and immunostaining	osteopontin, bisphosphonate [2-(2-pyridinyl)ethylidene-BP] (PEBP), alkaline phosphatase (ALP)	34, 58
	enzyme activity	**alkaline phosphatase**	
	gene level	**runt-related transcription factor 2** [Runx2 or core binding protein A-1 (CBFA-1)], **osterix** (OSX), **osteocalcin** (OCN), **osteopontin** (OPN), **bone sialoprotein** (BSP), alkaline phosphatase, integrin-binding sialoprotein (IBSP), bone γ-carboxyglutamate protein (BGLAP)	34, 58−61
	dye staining	**Alizarin Red staining** (calcium)	62
	mineral deposition	**von Kossa staining** (calcium phosphate)	57, 60
2. Chondrocytes	protein level (immunostaining)	**collagen type II** (Col II), **collagen type X** (Col X), **aggrecan** (AGN), Sox-9, chondroitin-4-sulfate, chondroitin-6-sulfate, sulphated glycosaminoglycans	56, 57, 63−68
	glycosaminoglycan assay	glycosaminoglycan content	
	dimethylmethylene blue (DMMB) assay	proteoglycan (PG) content	69
	hydroxyproline assay	collagen content	65
	gene level	**collagen II**, collagen IX (Col IX), **collagen X**, collagen XI (Col XI), **aggrecan**, Sox 5, Sox 6, **Sox 9**, **cartilage oligomeric protein** (COMP), xylosyltransferase I (XT-1), α-4-*N*-acetylhexosaminyltransferase (EXTL2), β-1,4-*N*-acetylgalactosaminyltransferase (GalNAcT), glucuronyl C5 epimerase (GlcACSE)	63, 64, 67, 70−73
	dye staining	**Safanin O staining (proteoglycan)**, **Alcian blue staining (proteoglycan)**, EVG-staining, Masson's trichrome staining	34, 62, 64, 67, 70, 72
3. Adipocytes	morphology	round shape cells tends to differentiated into adipocytes	53, 54
	protein level	vimentin, adipocyte lipid-binding protein (ALBP)	53, 74
	enzyme activity	glycerol-3-phosphate dehydrogenase activity	75
	gene level	PPARγ, aP-2	61
	staining	Oil red O and Nile red staining for lipid droplet	62
4. Neural cells	morphology	neuronal-like cells having long neurites	76
	protein level	nestin, neuron-specific class III β-tubulin (TuJ1), galactosylceramidase (GalC), glial fibrillary acidic protein (GFAP), β-tubulin-III, microtubule-associated protein 2 (MAP2), O4, tyrosine hydroxylase (TH), neurofibromatosis (NFM), neurone-specific enolase (NSE)	76−81
	gene level	nestin, Musashi 1, neuron-specific class III β-tubulin (TuJ1), glial fibrillary acidic protein, microtubule-associated protein 2, Sox1, Sox2, CD133, tyrosine hydroxylase, neurofibromatosis, Nurr1, dopamine transporter (DAT), dihydropyrimidinase-related protein 2 (DRP-2), purine-sensitive aminopeptidase (PSA)	11, 61, 76, 81, 82
5. Cardiomyocytes	morphology	contractile cells	
	protein level	**cardiac troponin T (cTnT)**, **desmin**, myosin light chain (MLC), myosin heavy chain (MHC)	81
	gene level	Nkx2.5, GATA-4, MYH-6, TNNT2, TBX-5, myosin light chain (Mlc2a, MLC-2 V), tropomyosin, cTnI, ANP, **desmin**, **myosin heavy chain** (α-MHC, **β-MHC**), **cardiac troponin T**, Isl-1, and Mef2c	11
	electrocardiogram	electrocardiogram	
6. Smooth muscle cells	protein level	α-smooth muscle actin (ASMA), h1-calponin (CALP), SM2	83
	gene level	α-smooth muscle actin, h1-calponin, caldesmon, Smemb, SM22α, SM1, SM2	83
7. Epidermis	protein level	keratin 10 (early marker), filaggrin (intermediate marker), involucrin (late marker)	84
	gene level	keratin 10 (early marker), filaggrin (intermediate marker), involucrin (late marker)	84
8. Hepatocyte	morphology	oval cell morphology, small round cell morphology	46

dx.doi.org/10.1021/cr3001691 | *Chem. Rev.* 2012, 112, 4507−4540

Table 2. continued

differentiation lineage	characterization	specification	ref (example)
	protein level	CXCR4 (endoderm), α-fetoprotein (AFP), albumin (ALB), asialoglycoprotein receptor (ASGPR), cytochrome P450 (CYP_1A_1), hepatocyte nuclear factor-1α (HNF-1α), hepatocyte nuclear factor-3β (HNF-3β), hepatocyte nuclear factor-4α (HNF-4α), CCAAT-enhancer binding protein α (C/EBPα), cytokeratin-18 (CK18), cytokeratin-19 (CK19), low-density lipoprotein (LDL), GATA4	46, 51, 52, 86, 87, 113
	gene level	Sox17 (endoderm), Foxa2 (endoderm), Gata6 (endoderm), α-fetoprotein, albumin, hepatocyte nuclear factor-1α, hepatocyte nuclear factor-3β, hepatocyte nuclear factor-4α, cytokeratin 18, cytokeratin-19, asialoglycoprotein receptor, tryptophan oxygenase (TO), cytochrome P450 (CYP1A1, CYP2B6), CCAAT-enhancer binding protein α, glucose 6-phosphate (G6P), GATA4	46, 51, 52, 86, 87, 113
	urea assay	urea production	46, 51, 113
	albumin assay	albumin production	52, 86, 113
	glycogen assay	glycogen production	46, 52, 113
	α-fetoprotein assay	α-fetoprotein production	52, 86
	pentoxyresorufin (PROD) assay	cytochrome P450 activity	113
	staining	periodic acid–Schiff (PAS) staining for glycogen storage	46, 113

immunostaining. Mature neurons express neuron-specific class III β-tubulin (Tuj1), microtubule-associated protein 2 (MAP2), neuron-specific enolase (NSE), and purine-sensitive aminopeptidase (PSA). Oligodendrocytes express galactosylceramidase (GalC) and O4. Dopaminergic neurons express tyrosine hydroxylase (TH), neurofibromatosis (NFM), and dopamine transporter (DAT). Nerve cells are electrically excitable cells that transmit information by electrical and chemical signaling. Therefore, electrical and action potentials in nerve cells can be monitored using electrodes.

3. PREPARATION OF CULTURE MATRIX

Biomimetic stem cell cultures can be categorized as two-dimensional (2D) or three-dimensional (3D). 2D culture is useful for basic research to investigate the fundamental interactions between cells and immobilized nanosegments on dishes, but 3D culture of stem cells in biomaterials is essential for clinical applications. Figure 3 shows some examples of biomaterial designs for carrying stem cells, as well as direct injection of biomaterials without cells. The injection of hydrogels or scaffolds containing stem cells is categorized as 3D cultures. Cell sheets prepared on a surface-grafting polymer having low critical solution temperature (LCST), such as poly(*N*-isopropylacrylamide) (poly(NIPAM)), can be prepared on 2D dishes.[94,95] Recently, patch sheets of immobilized antibodies or ligands targeting specific stem cells, which recruit the stem cells from the patient's body, are reported to be effective in gathering autologous stem cells at sites of injury.[40] The following sections describe methods for (a) surface immobilization of ECM proteins and ECM-mimicking peptides on 2D culture dishes and (b) preparing hydrogels or scaffolds containing ECM proteins and ECM-mimicking peptides for 3D culture of stem cells.

3.1. ECM Immobilization on 2D Dishes

Typically, 2D cell culture dishes are coated with ECM proteins or ECM-mimicking peptides. Tables 3 and 4 show examples of the ECM proteins and ECM-mimicking peptides used to coat culture dishes and their binding sites on stem cells.[16,18,53,58,71, 83,91,96–118] Collagen types I, II, and IV, gelatin, laminin, laminin-1, laminin-5, vitronectin, and fibronectin are typically used as coating materials.[58,71,83,91, 96–98,100–102] ECM-mimicking peptides (e.g., RGD, DGEA, YIGSR, IKVAV, KRSR, P15, and GFOGER) are commonly used as coating or grafting materials.[16,18,53,97,103–118] Covalent binding is preferable for long-term effects in culture, but noncovalent coating is the simplest method for the preparation of dishes with immobilized ECM proteins or ECM-mimicking peptides. Figure 4 summarizes typical surface reactions for the covalent immobilization of ECM proteins and peptides on dishes. Proteins and ECM-mimicking peptides should be used in aqueous solution, as they are unstable biomolecules. Reactions between amino groups and between amino groups and carboxylic acids can be used to bind ECM proteins and ECM-mimicking peptides to plastic dishes. These plastic surfaces should therefore have amino groups, carboxylic acid groups, or hydroxyl groups to bind and immobilize ECM proteins or peptides. For dishes made of polyesters, such as poly(ε-caprolactone) (PCL), poly(glycolic acid) (PGA), poly(lactic acid) (PLA), or poly(lactic acid-*co*-glycolic acid) (PLGA), treatment with a diamine, such as hexamethylene diamine, generates amino groups on the surface by an aminolysis reaction. Then, ECM proteins and ECM-mimicking

dx.doi.org/10.1021/cr3000169 | *Chem. Rev.* 2012, 112, 4507–4540

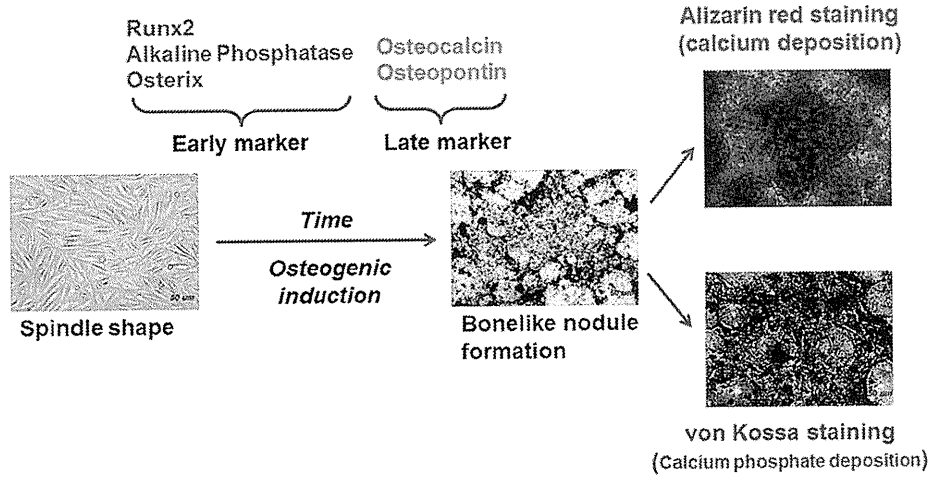

Figure 2. Osteogenic differentiation of MSCs, gene expression, and mineral deposition at early and late stages.

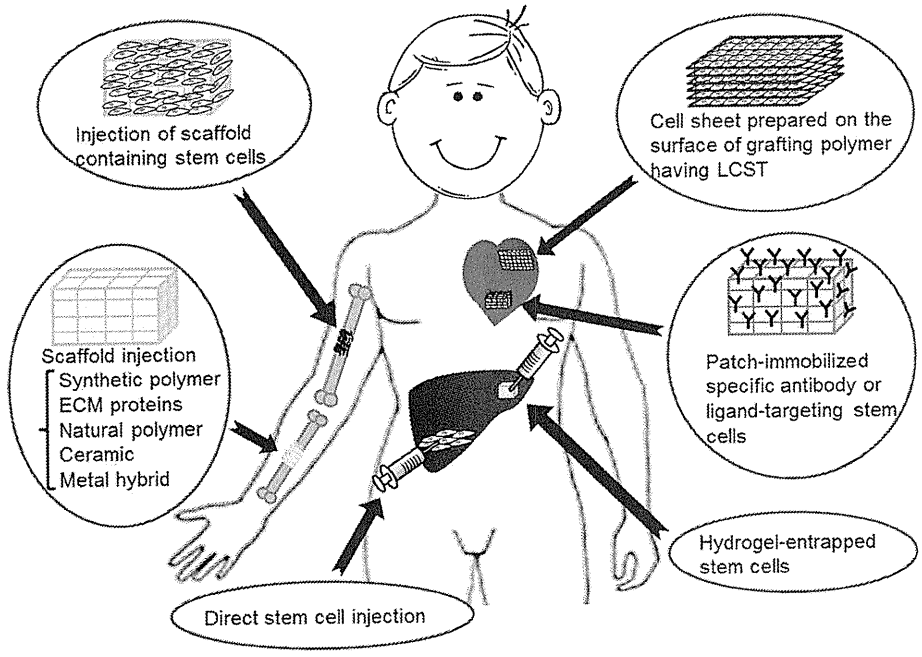

Figure 3. Some examples of biomaterial designs with and without stem cells for the injection of biomaterials in clinical applications: (a) injection of scaffold containing stem cells, (b) injection of scaffold without cells, (c) direct stem cell injection, (d) injection of cell sheets, (e) injection of patch-immobilized specific antibody or ligand-targeting stem cells, and (f) injection of hydrogel-entrapped stem cells.

peptides can be covalently immobilized using hexamethylene diisocyanate (HMDIC), 1,6-dimethyl suberimidate dihydrochloride (DMS),[119] or NHS/EDC reagent,[18] where NHS is *N*-hydroxysuccinimide and EDC is *N*-(3-dimethylaminopropyl)-*N*′-ethylcarbodiimide (Figure 4). EDC is a water-soluble carbodiimide that is generally used in the 4.0–6.0 pH range. Therefore, it is possible to immobilize ECM proteins and ECM-mimicking peptides in aqueous solution using NHS/EDC reagents. The covalent bonding between amino groups can be reacted with aqueous DMS.[119]

Genipin is generally used to cross-link proteins, such as collagen and gelatin, and chitosan via amino groups.[120,121] Genipin can also be used for the immobilization of ECM proteins and peptides on the surface of culture dishes with amino groups (Figure 4). NHS/EDC, DMS, and genipin are the recommended reagents to covalently immobilize ECM proteins and ECM-mimicking peptides on culture dishes.

3.2. 3D Culture in Hydrogels

Hydrogels are physically or chemically cross-linked polymer networks that are able to absorb large amounts of water. Injectable hydrogels containing stem cells can be delivered to sites of damage in patients with minimal invasiveness, and the hydrogels ensure that stem cells remain localized to the damaged sites more effectively than injected cells alone. Physical cross-linking is performed on ECM proteins with thermosensitive properties of lower critical solution temperature (LCST) or upper critical solution temperature (UCST), such as collagen and gelatin. Collagen can be dissolved in aqueous solutions at low temperature and forms gels at ~37 °C because of its LCST characteristics, and gelatin can be dissolved in aqueous solution at high temperatures and forms gels at room temperature because of its UCST. Therefore, stem cells can be dissolved in ECM protein solutions and efficiently entrapped in ECM gels at 20–37 °C. However, most ECM

dx.doi.org/10.1021/cr3000169 | *Chem. Rev.* 2012, 112, 4507–4540

Table 3. ECM Immobilized on Dishes for Adhesion, Differentiation, And Proliferation of Stem Cells and Some Examples of the Literature

ECM	binding site of cells	ref
collagen I	integrin ($\alpha V\beta 3$, $\alpha 2\beta 1$)	58, 96
collagen I	integrin ($\alpha 1\beta 1$)	97
collagen I	integrin ($\alpha 1\beta 1$, $\alpha 2\beta 1$, $\alpha 3\beta 1$)	71
collagen II	integrin ($\alpha 1\beta 1$, $\alpha 2\beta 1$, $\alpha 10\beta 1$)	71, 91
collagen IV	integrin ($\alpha 2\beta 1$, CD44)	98
gelatin		99
fibronectin	integrin ($\alpha 4\beta 1$, $\alpha 5\beta 1$, $\alpha V\beta 3$, $\alpha IIb\beta 3$, $\alpha V\beta 6$, $\alpha V\beta 5$)	58, 96
laminin	integrin ($\alpha 1\beta 1$, $\alpha 2\beta 1$, $\alpha 3\beta 1$, $\alpha 6\beta 1$, $\alpha 6\beta 4$)	100
laminin-1 (laminin 111)	integrin ($\alpha 1\beta 1$, $\alpha 2\beta 1$, $\alpha 6\beta 1$, $\alpha 7\beta 1$, $\alpha 9\beta 1$), α-dystroglycan, suifade, and heparan sulfate proteoglycan	83, 101
laminin-5 (laminin 332)	integrin ($\alpha 2\beta 1$, $\alpha 3\beta 1$, $\alpha 6\beta 1$, $\alpha 6\beta 4$)	102
laminin-10/11	integrin ($\alpha 3\beta 1$, $\alpha 6\beta 1$, $\alpha 6\beta 4$)	100
vitronectin	integrin ($\alpha V\beta 3$, $\alpha V\beta 5$)	58, 96

proteins and ECM-derived oligopeptides (ECM peptides) need other forms of cross-linking to trap stem cells and generate hydrogels. Typically, photocross-linking and chemical cross-linking of ECM proteins and ECM peptides are used. There are several excellent reviews that discuss hydrogel preparation and reaction in detail.[12,14] Therefore, this section deals briefly with the preparation of ECM hydrogels using photocross-linking and chemical cross-linking with cross-linking agents. The application of ECM hydrogels containing stem cells is discussed in section 5 for specific ECM proteins and ECM peptides.

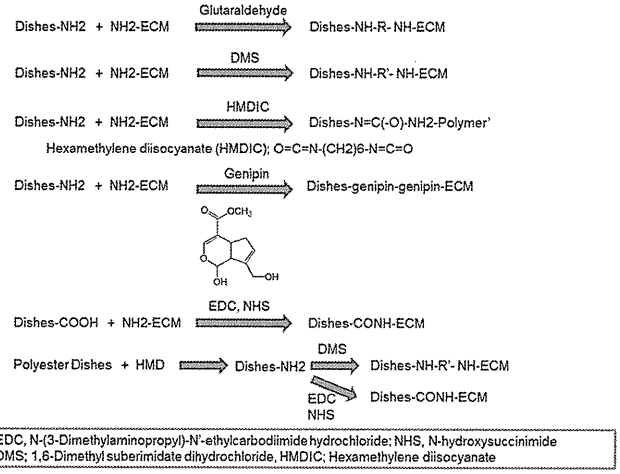

Figure 4. Surface reactions of covalent immobilization of ECM proteins and ECM-mimicking peptides on dishes.

3.2.1. Photocross-Linking of ECM Proteins and ECM Peptides. Hydrogels containing stem cells can be easily prepared by UV irradiation of ECM proteins and ECM–peptide solutions. These preparations can be used as injectable hydrogels via photocross-linking. However, it is first necessary to introduce double bonds into ECM proteins and ECM peptides for photocross-linking. ECM proteins and ECM peptides have $-OH$, $-NH_2$, and $-COOH$ functional groups. Double bonds can be introduced into ECM proteins and ECM

Table 4. ECM-Mimicking Peptides Immobilized on Dishes for Adhesion, Differentiation, And Proliferation of Stem Cells

ECM-mimicking peptide	ECM proteins for mimicking	binding site of cells	ref
DGEA	collagen I	integrin ($\alpha 2\beta 1$)	103–105
GTPGPQGIAGQRGVV (P15)	collagen I	integrin ($\alpha 2\beta 1$)	103, 106
$(RADA)_4$GG**DGEA**	collagen I	integrin ($\alpha 2\beta 1$)	116
$(RADA)_4$GGFPGERGVEGPGP	collagen I		116
GFOGER	collagen	integrin ($\alpha 2\beta 1$)	103, 107, 108
MNYYSNS	collagen IV		109
RGD	collagen I	integrin ($\alpha V\beta 3$)	97, 110
ELIDVPST (CS-1)	fibronectin	integrin ($\alpha 4\beta 1$); VLA-4	16, 111
FN-40	fibronectin	integrin ($\alpha 4\beta 1$, VLA-4)	16, 112
FN-120	fibronectin	integrin ($\alpha 5\beta 1$); VLA-5	16, 112
FN–CH296	fibronectin	integrin ($\alpha 4\beta 1$, $\alpha 5\beta 1$)	16, 112
KGGAVTG**RGD**SPASS	fibronectin	integrin ($\alpha 5\beta 1$); VLA-5	18, 113
GRGDSPK	fibronectin	integrin ($\alpha 5\beta 1$); VLA-5	18, 113
KNNQKSEPLIGRKKT	fibronectin	heparin-binding domain	53
RGDS	fibronectin		109
PHSRN	fibronectin		109
KYGAAS**IKVAV**SADR	laminin		18, 114
YIGSR	laminin		109
IKVAV	laminin		115
PPFLMLLKGSTR	laminin-5 (laminin332)	integrin ($\alpha 3\beta 1$)	
(RADA)4-GG**PDSGR**	laminin		116
(RADA)4-GGSDPG**YIGSR**	laminin		116
(RADA)4-GGIKVAV	laminin		116
KGGPQVT**RGD**VFTMP	vitronectin	integrin ($\alpha V\beta 5$)	18, 117
KGGNGEP**RGD**TYRAY	bone sialoprotein (BSP)		18, 118
PEO4-NGEP**RGD**TYRAY	BSP-linker		18, 118
RGD	osteopontin	integrin ($\alpha V\beta 3$)	97

dx.doi.org/10.1021/cr3000169 | Chem. Rev. 2012, 112, 4507–4540

peptides by the reactions of acryloyl chloride,[122] glycidyl methacrylate,[12,123] and 2-aminoethylmethacrylate[12,124] (Figure 5). Figure 5 also shows a schematic for preparation method of

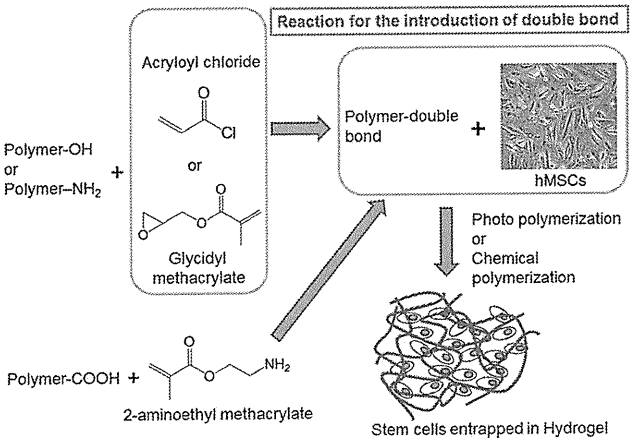

Figure 5. Schematic of the preparation method of hydrogels with entrapped stem cells by photopolymerization.

hydrogels with entrapped stem cells by photopolymerization. Aqueous solutions containing stem cells and macromers of ECM proteins and ECM peptides are irradiated with UV light to generate hydrogels with entrapped stem cells.

Poly(ethylene glycol)diacrylate (PEODA) is typically added to the reaction solution to generate optimal hydrogels.[65,125−129] Yang et al. prepared PEODA hydrogels incorporating RGD adhesive peptides and goat BMSCs by photopolymerization. They found that RGD-conjugated PEODA hydrogels promoted the osteogenic differentiation of BMSCs, and RGD enhanced differentiation in a dosage-dependent manner, with the highest concentration (2.5 mM) in the reaction solution being optimal in their study.[125]

3.2.2. Chemical Cross-Linking of Hydrogels. Hydrogels of ECM proteins can also be prepared by chemical cross-linking. Similar to ECM protein immobilization on 2D dishes, as discussed in section 3.1, NHS/EDC, DMS, HMDIC, and genipin are typically used as cross-linking agents. Glutaraldehyde is not commonly used for the preparation of hydrogels in tissue engineering because it is relatively toxic to stem cells. DMS, HMDIC, and genipin allow cross-linking between amino groups, whereas NHS/EDC leads to cross-linking between carboxylic acids and amino groups in ECM proteins.

Chang et al. compared gelatin hydrogels cross-linked with genipin and gelatin hydrogels cross-linked with glutaraldehyde.[120] They found that the degree of inflammatory reaction in wounds treated with the genipin-cross-linked gelatin was significantly less severe than those covered with the glutaraldehyde-cross-linked gelatin in vivo.[120] In addition, the healing rates of wounds treated with the genipin-cross-linked gelatin were notably faster than those with glutaraldehyde-cross-linked hydrogels.[120]

3.3. 3D Culture in Scaffolds

Scaffolds seeded with stem cells can support 3D tissue formation artificially. It is optimal for scaffolds (a) to allow cell attachment and migration, (b) to allow diffusion of nutrients, growth factors, and waste secreted by cells, and (c) to have mechanical properties similar to the natural tissue. Most of the scaffolds have high porosity (>80%) and large pore size (200−800 μm), which allow diffusion of nutrients, growth factors, and waste, but these properties also lead to weak mechanical properties. Biodegradability of scaffolds is often required because scaffolds should be absorbed by the surrounding tissues without the necessity of surgical removal. It is preferable that the degradation rate of scaffolds should be matched to the speed of tissue formation. The degradation speed of scaffolds can be regulated by the degree of cross-linking. Scaffolds prepared from ECM proteins and ECM peptides are desirable because of their biodegradable characteristics. ECM proteins used for the preparation of scaffolds are typically collagen type I, collagen type II, gelatin, fibronectin, laminin, and vitronectin. ECM proteins can be used as (a) coating materials, (b) blending materials, and (c) main materials of scaffolds.

3.3.1. Preparation of Scaffolds. There are several methods used to prepare scaffolds for tissue engineering and 3D culture of stem cells, including (a) freeze-drying, (b) salt leaching, (c) porogen leaching, (d) use of nonwoven fabric or mesh, (e) nanotopography, and (f) electrospinning. In the freeze-drying method, ECM proteins are dissolved in a buffer solution. The ECM solution is frozen at −20 or −80 °C and then lyophilized in a freeze-dryer before being washed and stored (Figure 6). If necessary, the scaffolds are also cross-linked.

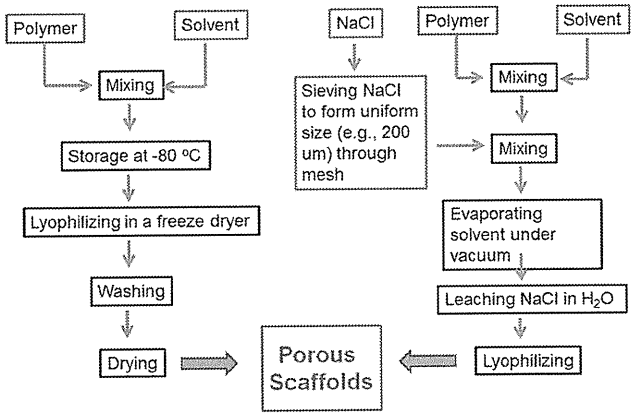

Figure 6. Typical preparation method of porous scaffolds by freeze-drying (a) and salt leaching (b).

The salt-leaching method is as follows. Biopolymers and/or ECM proteins are dissolved in a solvent. Salt, typically NaCl, is sieved to generate a uniform distribution of size using filtration through mesh and added into the solution. The solvent of the solution is vaporized under vacuum to generate dry scaffolds. Salt is then leached from the scaffolds by immersion in water after drying the scaffolds (Figure 6). The porogen-leaching method is a similar method to the salt-leaching method, but other uniformly sized particles, such as polymeric particles, are used instead of salt.

3.4. 3D Culture in Nanofibers

Peptide amphiphiles (PAs), which have a hydrophilic domain and a hydrophobic domain, are known to spontaneously generate self-assembled nanofibers above critical micelle concentrations.[109,116,130] MSC differentiation on self-assembled nanofibers using ECM peptides is discussed in section 5.8.1.

A typical method to create nanofibers is electrospinning. Electrospun scaffolds can support cell adhesion and growth and

dx.doi.org/10.1021/cr3000169 | Chem. Rev. 2012, 112, 4507−4540

promote differentiation of stem cells.[131] Nanofibers can be generated from a spinning nozzle when high voltage is applied between the spinning nozzle and a flat metal collector. Typical electrospinning products are flat and highly interconnected scaffolds with a nonwoven fabric sheetlike morphology. These characteristics hinder cell infiltration and growth throughout the scaffolds. Blakeney et al. have developed a three-dimensional cotton ball-like electrospun scaffold that consists of low-density, uncompressed nanofibers.[131] A grounded spherical dish and an array of needle-like probes were used instead of a traditional flat-plate collector to create a cotton ball-like scaffold. Scanning electron microscopy showed that the cotton ball-like scaffold consisted of electrospun nanofibers with a similar diameter, but with larger pores and less dense structures than traditional electrospun scaffolds.[131] The cotton-ball like scaffolds prepared from ECM proteins by electrospinning will be interesting for use as scaffolds for guiding specific lineages of stem cell differentiation.

4. PHYSICAL PROPERTIES OF BIOPOLYMERS (BIOMATERIALS) GUIDE STEM CELL DIFFERENTIATION FATE (LINEAGE)

The interactions between MSCs and ECM proteins are classified as physical, chemical, and biological. It has recently been recognized that stem cell differentiation is directed by physical properties of culture materials as well as by biochemical responses to growth factors and ECM proteins.[19,20,132] Cells in bone, muscle, liver, and brain tissues reside in different environments that have diverse physical properties.[133] The matrix stiffness for differentiated cells is known to influence focal-adhesion structure and the cytoskeleton.[134−139] Engler et al. reported that soft materials, with similar stiffness to the brain, tend to differentiate MSCs into neurogenic cells, whereas stiffer materials that mimic muscle guide MSCs into myogenic cells and rigid materials similar to collagenous bone induce osteogenic differentiation (Figure 7).[19] However, this work was performed on a 2D surface of hydrogels coated with collagen. The effect of stiffness in 3D culture may produce different results than in 2D culture.

Gilbert et al. also reported that the elasticity of culture materials regulates self-renewal of skeletal muscle stem cells.[20]

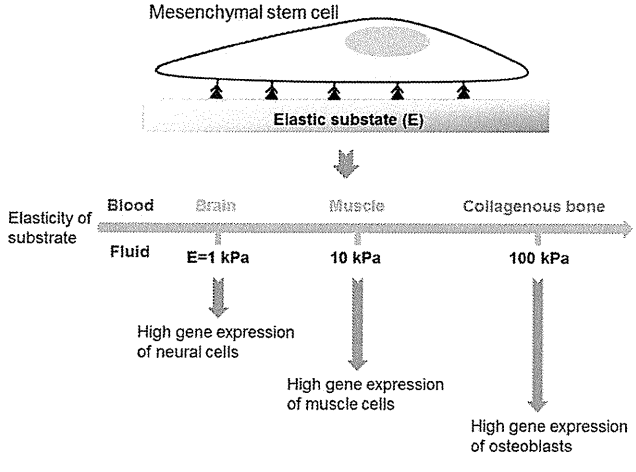

Figure 7. Physical properties decide the fate of stem cell cultured on biomaterials with different elasticity. Modified with permission from ref 19. Copyright 2006 Elsevier Inc.

Muscle stem cells (MuSC's) exhibit robust regenerative capacity in vivo, but this capacity is rapidly lost in culture. They showed that the elasticity of culture materials was a potent regulator of MuSC fate. MuSC's cultured on soft hydrogel substrates that mimicked the elasticity of muscle (12 kPa) self-renew in vitro and contributed extensively to muscle regeneration when transplanted into mice, unlike MuSC's grown on rigid plastic dishes (~106 kPa), as shown by histology and bioluminescence imaging. These studies provide evidence that propagation of adult muscle stem cells is possible by recapitulating physiological tissue rigidity.[20] This finding may contribute to future cell-based therapies for muscle-wasting diseases.

The effect of physical interactions between MSCs and culture materials on stem cell fate is discussed in several articles.[19,20,61,133,140−154] Some landmark findings are summarized in Table 5, and some examples of physical effects on differentiation of MSCs cultured on ECM proteins are reviewed here.

Table 5. Some Articles Discussing Physical Effect of Substrates on Differentiation of MSCs Cultured on the Substrates

authors	contents	ref (year)
J. R. Mauney et al.	**mechanical stimulation** promotes osteogenic differentiation of hBMSCs	140 (2004)
J. S. Park et al.	differential effects of **equiaxial and uniaxial strain** on MSCs	141 (2004)
V. E. Meyers et al.	**microgravity** disrupts collagen I/integrin signaling during osteogenic differentiation of hMSCs	142 (2004)
V. I. Sikavitsas et al.	**flow perfusion** enhances the calcified matrix deposition of marrow stromal cells in scaffolds	143 (2005)
H. Hosseinkhani et al.	**perfusion culture** enhances osteogenic differentiation of MSCs	144 (2005)
A. J. Engler et al.	**matrix elasticity** directs stem cell lineage specification	19 (2006)
R. D. Sumanasinghe et al.	osteogenic differentiation of hMSCs in collagen matrices: effect of **uniaxial cyclic tensile strain**	145 (2006)
D. F. Ward et al.	**mechanical strain** promotes osteogenic differentiation of hMSCs	61 (2007)
E. K. F. Yim et al.	**nanostructures** inducing differentiation of hMSCs into neurinal lihneage	154 (2007)
B. Lanfer et al.	growth and differentiation of MSCs on **aligned collagen** matrices	146 (2009)
Q. Li et al.	ECM with the **rigidity** of adipose tissue helps adipocytes maintain insulin responsiveness	147 (2009)
M. Zscharnack et al.	**low O_2** expansion improves subsequent chondrogenesis of BMSCs in hydrogel	148 (2009)
C. H. Huang et al.	interactive effects of **mechanical stretching** and ECM proteins on initiating osteogenic differentiation of hMSCs	149 (2009)
P. M. Gilbert et al.	substrate **elasticity** regulates skeletal muscle stem cell self-renewal in culture	20 (2010)
G. C. Reilly and A. J. Engler	intrinsic ECM properties regulate stem cell differentiation (**mechanobiology**)	150 (2010)
J. M. Kemppainen and S. J. Hollister	differential effects of **designed scaffold** permeability on chondrogenesis by BMSCs	151 (2010)
E. K. F. Yim et al.	**nanotopography**-induced changes in focal adhesions, cytoskeletal organization, and mechanical properties of hMSCs	152 (2010)
J. Tang et al.	regulation of stem cell differentiation by cell−cell contact on **micropatterned** material surfaces	153 (2010)
P. A. Janmey and R. T. Miller	mechanisms of **mechanical** signaling in development and disease	133 (2011)

dx.doi.org/10.1021/cr3000169 | Chem. Rev. 2012, 112, 4507−4540

4.1. Mechanical Stretching Effect of Culture Surface-Coated with ECM Proteins

Mechanical strain and ECM proteins play important roles in the osteogenic differentiation of hMSCs.[61,140,145,149] Several studies have shown that mechanical strain can promote osteogenic or other lineage differentiation in cells cultured on ECM proteins even in the absence of osteogenic supplements in the culture medium.[61,145,149]

Park et al. reported that mechanical strain regulated the expression of vascular smooth muscle cell (SMC) markers in MSCs (Figure 8).[141] Cyclic equiaxial strain downregulated smooth muscle (SM) α-actin and SM-22α in MSCs on collagen- or elastin-coated membranes after one day and decreased the level of α-actin in stress fibers. In contrast, cyclic uniaxial strain transiently increased the expression of SM α-actin and SM-22α after one day, which subsequently returned to basal levels after the cells aligned in the direction perpendicular to the strain.[141] In addition, uniaxial but not equiaxial strain induced a transient increase in collagen type I expression. DNA microarray experiments showed that uniaxial strain increased SMC markers and regulated the expression of matrix molecules without significantly changing the expression of differentiation markers (e.g., ALP and collagen type II) in other cell types.[141] Their results suggest that uniaxial strain, which better mimics the type of mechanical strain experienced by SMCs, could promote MSC differentiation into SMCs if cell orientation is controlled.[141]

Ward et al. showed that application of a 3−5% tensile strain to a collagen type I substrate stimulated osteogenesis in attached hMSCs through gene focusing via a MAPK signaling pathway.[61] They found that mechanical strain led to an increase in the expression of osteogenic marker genes while simultaneously reducing expression of marker genes from three alternate lineages (chondrogenic, adipogenic, and neurogenic).[61] Mechanical strain also increased matrix mineralization (a hallmark of osteogenic differentiation) and activation of extracellular signal-related kinase 1/2 (ERK).[61] These results demonstrated that mechanical strain enhanced collagen type I-induced gene focusing and osteogenic differentiation in hMSCs through the ERK/MAPK signaling pathway.[61]

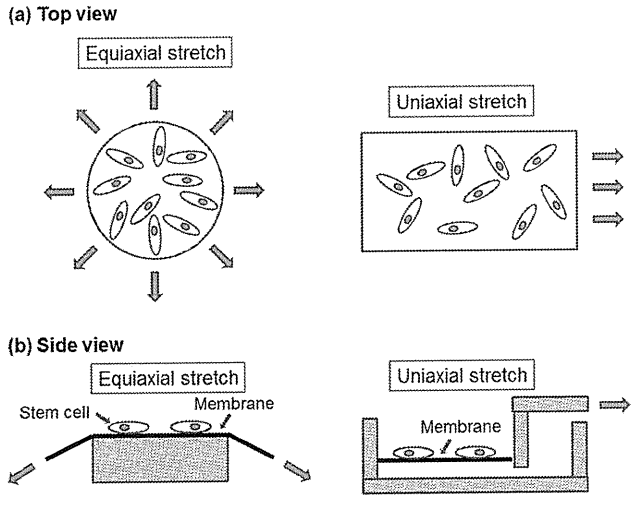

Figure 8. Schematic model of the apparatus that can apply equiaxial (a) and uniaxial (b) strain to MSCs. Modified with permission from ref 141. Copyright 2004 Wiley Periodicals.

Huang et al. investigated the combined effects of ECM proteins and mechanical factors (cyclic stretching) in driving hMSCs toward osteogenic differentiation.[149] hMSCs cultured in regular medium were grown on substrates coated with various ECM proteins (collagen type I, vitronectin, fibronectin, and laminin) and subjected to cyclic mechanical stretching.[149] All of the ECM proteins tested supported hMSC differentiation into osteogenic phenotypes in the absence of osteogenic supplements.[149] Cyclic mechanical stretching activated the phosphorylation of focal adhesion kinase (FAK), induced upregulation of the transcription and phosphorylation of Runx2, and subsequently increased ALP activity and mineralized matrix deposition.[149] Fibronectin and laminin exhibited greater effects of supporting stretching-induced osteogenic differentiation than did collagen type I and vitronectin.[149] It was suggested that the ability of ECM proteins and mechanical stretching to regulate osteogenesis in hMSCs may be exploited in bone tissue engineering by appropriate matrix design and by mechanical stimulation.[149]

4.2. Low Oxygen Expansion Promotes Differentiation of MSCs

Several groups have reported the effects of low oxygen tension on the differentiation of MSCs, especially in chondrogenic differentiation of MSCs cultured on ECM substrates.[148,155] Zscharnack et al. investigated the effect of low oxygen tension (5%) during the expansion of ovine MSCs on colony-forming unit-fibroblast (CFU-F) formation and chondrogenesis in pellet culture and in collagen type I hydrogels.[148] MSCs expanded in 5% O_2 showed a 2-fold higher CFU-F potential, and chondrogenic differentiation was enhanced in both pellet culture and collagen type I hydrogels. It was demonstrated that physiologically low oxygen tension during monolayer expansion of ovine MSCs was advantageous to improving cartilage tissue engineering in a sheep model.[148]

4.3. Other Physical Effect Affecting Differentiation of MSCs

There are several other physical effects that promote differentiation of MSCs on ECM protein surfaces. (i) Perfusion culture promotes osteogenic differentiation of MSCs cultured on ECM protein surface.[143,144] (ii) Microgravity disrupts collagen type I/integrin signaling during osteoblastic differentiation of hMSCs.[142] (iii) The mechanical properties of ECM proteins guide specific lineage differentiation of MSCs.[147,150,156,157] (iv) The topography of ECM proteins promotes differentiation of MSCs cultured on aligned or patterned substrates.[74,146,151−154,158]

5. MSC CULTURE ON ECM PROTEINS AND NATURAL BIOPOLYMERS

The ECM is the extracellular component of animal tissues that provides structural support for the cells, in addition to stimulating various important biological functions. ECM proteins are able to dictate whether cells will proliferate or undergo growth arrest, migrate or remain stationary, and thrive or undergo apoptotic death.[159] Therefore, the ECM proteins are an important factor in reproducing the biological niches of cells in vitro, which guides MSCs to differentiate into different lineages such as osteoblasts, chondrocytes, adipocytes, cardiomyocytes, neural cells, hepatocytes, and β-cells. The differentiation of MSCs in culture systems depends on the components, structure (morphology), origin, and quantity of ECM proteins that are used. Because ECM proteins are used as scaffolds for the organization of cells in tissues, ECM proteins

are the main cell culture materials used to control the proliferation and differentiation of MSCs in tissue engineering and regenerative medicine, both in vitro and in vivo. Therefore, this review focuses mainly on the differentiation of MSCs cultured on biomaterials made of specific ECM proteins and on the biological and chemical interactions between these cells and proteins.

5.1. Chemical and Biological Interactions of ECM Proteins and Stem Cells

ECM proteins have chemical functional groups of carboxylic acid, amine, phosphate, and/or sulfonic acid. They also have aspects of polyelectrolytes and characteristic isoelectric points (IEPs).[160−175] Table 6 shows the IEPs of some ECM proteins,

Table 6. Isoelectric Points of Some ECM Proteins, Growth Factors, And Polymers

materials	isoelectric point	ref
	ECM	
collagen type I	4.7, 6.4, 6.78, 7.02, and 8.26 depending on preparation conditions	172−174
gelatin sol	7.8, temp > 40, or increasing pH	344
gelatin gel	4.7, temp < 15, or decreasing pH	344
fibronectin	5.5−6.0	160
vitronectin	4.75−5.25	161
laminin	5.87, 4.89, and 5.08	162
heparin	3.4	163
hyaluronic acid	2.5	170
	growth factor	
FGF-1 (aFGF)	5.6	169
FGF-2 (bFGF)	9.6	169
rhBMP-2	9	171
insulin	5.3	168
PDGF	9.8	165
EGF	4.0−5.0	
TGF-β1	9.5	164
	polymer	
agarose	5.5	166
alginate	5.4	175
poly(lactic-*co*-glycolic acid) (PLGA)	2.75	163
poly(L-lysine)	9.5	163
chitosan	8.7	167
polyacrylamide	5.7	166

natural biopolymers, and growth factors.[160−172,174,175] IEPs are as follows: gelatin gel and collagen type I 4.7−8.3,[172,174] fibronectin 5.5−6.0,[160] laminin 4.9−5.9,[162] vitronectin 4.8−5.3,[161] heparin 4.7,[163] hyaluronic acid 2.5,[170] agarose 5.5,[166] and alginate 5.4.[175] Most ECM proteins and natural biopolymers are negatively charged under physiological conditions. The IEP of some growth factors is <7 (e.g., 5.6 for FGF-1[169] and 5.3 for insulin[168]), whereas for other growth factors, it is >7 (e.g., 9.6 for FGF-2,[169] 9.0 for BMP-2,[171] 9.8 for PDGF,[165] and 9.5 for TGF-β1[164]). Some binding between ECM proteins and growth factors (e.g., collagen type I and BMP-2) is mainly due to electrochemical interactions.

The binding of ECM proteins to cells is mainly mediated by integrin receptors. Integrins comprise a large family of cell-surface receptors that bind and mediate adhesion to ECM components, organize the cytoskeleton, and activate intracellular signaling pathways.[159] Each integrin consists of two type-1 transmembrane subunits: α and β. In mammals, 18 α- and 8 β-subunits associate in various combinations to form 24 integrin dimers that can bind to distinct subsets of ECM ligands.[176,177]

Most ECM proteins have molecular weights of 10−1000 kDa but only a few integrin-binding domains. These integrin-binding domains have specific sequences of a few amino acids (3−10), e.g., RGD, DGEA, YIGSR, IKVAV, and GFOGER. Table 4 summarizes the integrin receptors and amino acid sequences that mediate cell−ECM associations that are important for MSC proliferation and differentiation, as well as normal cell culture.

Many members of the integrin family, including $\alpha5\beta1$, $\alpha8\beta1$, αIIb$\beta3$, $\alpha V\beta3$, $\alpha V\beta5$, $\alpha V\beta6$, and $\alpha V\beta8$, recognize an Arg-Gly Asp (RGD) motif within fibronectin,[16,18,109] fibrinogen,[109] vitronectin,[18] von Willebrand factor, and other large glycoproteins. Collagen type I has a cell-binding domain of DGEA, which binds to integrin $\alpha2\beta1$.[103] Collagen type I is also bound by integrins $\alpha1\beta1$, $\alpha3\beta1$, and $\alpha V\beta3$.[58,97] RGD in collagen type I is reported to associate with integrin $\alpha V\beta3$.[97] The large size of ECM proteins, compared to the small integrin-binding motifs, provides not only structural support but also conformational regulation of the cell-binding domains. The differences in conformation of the cell-binding domains lead to different associations with specific integrin receptors.[178,179] MSC differentiation on culture materials composed of specific ECM and natural biopolymers is discussed in the following sections.

5.2. Collagen

Collagen is a typical ECM protein used in the culturing of MSCs, which is found in all animals, especially in the flesh and connective tissues of mammals.[180] Collagen is the main component of connective tissue and the most abundant protein in mammals,[181] making up ~25−35% of the whole-body protein content. Elongated collagen fibrils are found in fibrous tissues, including skin, ligaments, and tendons. Collagen is also abundant in the cornea, cartilage, bone, blood vessels, gut, and intervertebral discs. Because of its abundance, collagen, especially collagen type I, is relatively inexpensive compared to other ECM proteins such as laminin, vitronectin, and fibronectin, which allows us to use it in large quantities to make scaffolds and hydrogels for stem cell culture.[144,182−185]

To date, 29 types of collagen have been identified and described. The five most common types are (i) collagen type I (genes; COL1A1, COL1A2), which is the main component of bone and also found in skin and tendons; (ii) collagen type II (gene; COL2A), which is the main component of cartilage; (iii) collagen type III (gene; COL3A), which is the main component of reticular fibers; (iv) collagen type IV (genes; COL4A1, COL4A2, COL4A3, COL4A4, COL4A5, and COL4A6), which is found in basement membranes;[186] and (v) collagen type V (COL5A1, COL5A2, and COL5A3), which is found in placenta and hair.[187]

Collagen undergoes many post-translational modifications, including extensive cross-linking. Defective cross-linking has been implicated in human syndromes (e.g., osteogenesis imperfecta and Ehlers-Danlos syndrome).[188] However, it was reported that the inhibition of cross-linking of collagen was not required for osteogenic differentiation of hMSCs, as shown by the expression of ALP and genome-wide gene-expression analysis, but it did enhance matrix mineralization.[188] Specific characteristics of collagen, such as stiffness, elasticity, degree of cross-linking, and origin (i.e., cow-, pig-, or fish-derived collagen

dx.doi.org/10.1021/cr3000169 | Chem. Rev. 2012, 112, 4507−4540

from fetal or adult animals), might affect stem cell fate when it is used in the culture materials and scaffolds for MSC differentiation.

Collagen can form gels or scaffolds without elaboration. To prepare collagen gel, the protein is dissolved in acetic acid solution, and the solution is diluted with phosphate-buffered saline. After adjusting the pH of collagen solution to 7.4 by the addition of NaOH, the collagen solution is chilled in an ice bath to prevent gelation. Cells are then added into the collagen solution at the desired density, and the cell solution is incubated at 37 °C to allow gel formation. Once the gel has set, extra culture medium is added to the top of the gels and the cultures are returned to the incubator.[189] Tables 7 and 8 summarize several types of collagen materials and scaffolds for MSC differentiation that have been reported in the literature.[34,37,40,45,46,53,56,61,63,70,71,79,83,84,91,97,98,101,105,110,141,144,146,148,149,151,154,182−185,189−217]

5.2.1. Collagen Type I Scaffolds. Collagen sponges (scaffolds) can be fabricated by the conventional freeze-drying method followed by cross-linking.[144,202] Collagen type I is frequently used for scaffolds and culture materials to promote osteogenic[105,182,183,190,193,218] and chondrogenic[183] differentiation of MSCs.

Many reports have focused on the osteogenesis of MSCs cultured on collagen type I scaffolds,[105,183] because collagen type I is a major organic component of bones.[91] Activation of specific integrins ($\alpha1\beta1$ and/or $\alpha2\beta1$) by collagen type I was reported to mediate the osteogenic response of hBMSCs (human BMSCs).[70,97,105,188,194]

The proliferation and differentiation of MSCs into osteoblasts on collage type I-coated dishes and scaffolds are promising. It was reported that the tissue culture dishes coated with collagen type I, but not fibronectin, laminin, gelatin, or poly L-lysine, enhanced late cell proliferation and promoted osteogenesis by hBMSCs, as evidenced by an increase in Alizarin Red S staining, ALP activity, and mRNA levels of Runx2 and osteocalcin.[192] Tsai et al. found that collagen type I coating induced the activation of extracellular signal regulated kinase (ERK) and Akt, but not FAK.[192] Antibody blocking of $\alpha2\beta1$ integrin did not inhibit collagen type I-induced osteogenesis of hBMSCs.[192] This result indicates that cell signaling via $\alpha2\beta1$ integrin is not required for osteogenesis of hBMSCs cultured on collagen type I.

Donzelli et al. reported osteogenic differentiation of rat MSCs in a commercially available collagen scaffold, Gingistat. MSC commitment to osteogenic differentiation was demonstrated by the expression of osteopontin and osteocalcin, as well as increased ALP activity. Nodular aggregates and Alizarin Red-stained calcium deposits were observed in MSCs induced toward osteogenic differentiation cultured in the collagen scaffold.[183]

A honeycomb structure of collagen scaffold was reported to promote BMSC proliferation and differentiation.[110] BMSCs on honeycomb collagen scaffolds were able to differentiate into osteoblasts even without osteogenic induction medium to some extent, as shown by ALP activity and observation of mineral deposition by von Kossa staining.[110]

In another study, collagen type I nanofibers were prepared by electrospinning and seeded with hBMSCs. The morphology, growth, adhesion, cell motility, and osteogenic differentiation of hBMSCs on nanosized fibers of varying diameters (50−200, 200−500, and 500−1000 nm) were examined. The cells on all the nanofibers had a more polygonal and flattened cell morphology than those on tissue culture polystyrene dishes (TCPSs). Moreover, hBMSCs grown on 500−1000 nm nanofibers had significantly higher cell viability than the TCPS control.[182] Sefcik et al. also prepared collagen type I scaffolds by the electrospinning method.[184] Osteogenic genes (collagen type I, ALP, osteopontin, osteonectin, osteocalcin, and Runx2) were reported to be upregulated (>1-fold) in adipose-derived stem cells (ADSCs) cultured on nanofiber

Table 7. Some Research Studies for Stem Cell Differentiation on 2D Collagen Materials

stem cell source[a]	material for stem cell culture	differentiation	ref
hBMSCs	collagen I (2D culture, coating on dishes)	osteoblasts	97, 149, 190−192
rat BMSCs	collagen I (2D culture, coating on dishes)	osteoblasts	193
rBMSCs	collagen I (2D culture, gel)	osteoblasts	194
mBMSCs	collagen I (2D culture, coating on dishes)	osteoblasts, adipocytes	195
hBMSCs	collagen I (2D culture, coating on dishes)	osteoblasts, adipocytes	196
hBMSCs	collagen I (2D culture, aligned collagen on dishes)	osteoblasts, adipocytes	146
hBMSCs	collagen I (2D culture, aligned heparin on collagen I matrix)	osteoblasts, adipocytes	146
pBMSCs	collagen I (2D culture, coating on dishes)	osteoblasts, adipocytes	197
hBMSCs	collagen I (2D culture, coating on dishes)	osteoblasts, chondrocytes	61
hADSCs	collagen I (2D culture, coating on dishes)	adipocytes	53
hESCs (TE03, TE06)	collagen I (2D culture, coating on dishes)	neural cells	79
hBMSCs	collagen I (2D culture, coating on dishes)	neural cells	101, 154,
mESCs	collagen I (2D culture, coating on dishes)	neural cells	198
monkey ESCs	collagen I (2D culture, coating on dishes)	mesoderm cells, endoderm cells	199
mouse hepatitic stem cells	collagen I (2D culture, coating on dishes)	hepatocytes	200
hBMSCs, hAFSCs	collagen I (2D culture, coating on dishes)	hepatocytes	46
human neural stem cells	collagen I (2D culture, coating on dishes)	oligogliocytes	37
teratocarcinoma stem cells (F9)	collagen I (2D culture, coating on dishes)	visceral endoderm cells	98
hBMSCs	collagen I (2D culture, coating on dishes)	vascular smooth muscle cells	141
mESCs	collagen I (2D culture, coating on dishes)	lung epithelium	201
hBMSCs	collagen IV (2D culture, coating on dishes)	osteoblasts	97
hADSCs	collagen IV (2D culture, coating on dishes)	adipocytes	53
hBMSCs	collagen IV (2D culture, coating on dishes)	neural cells	101
mouse hepatitic stem cells	collagen IV (2D culture, coating on dishes)	hepatocytes	200
teratocarcinoma stem cells (F9)	collagen IV (2D culture, coating on dishes)	visceral endoderm cells	98
hBMSCs	collagen IV (2D culture, coating on dishes)	smooth muscle cells	200

[a]ADSC's, adipose-derived stem cells; BMSCs, bone marrow stem cells; ESCs, embryonic stem cells; hBMSCs, human BMSCs; rBMSCs, rabbit BMSCs; mBMSCs, mice BMSCs; pBMSCs, porcine BMSCs; hADSCs, human ADSCs; hESCs, human ESCs; mESCs, mice ESCs; hAFSCs, human amniotic fluid-derived stem cells.

dx.doi.org/10.1021/cr3000169 | Chem. Rev. 2012, 112, 4507−4540

Table 8. Some Research Studies for Stem Cell Differentiation on 3D Collagen Materials

stem cell source[a]	material for stem cell culture[b]	differentiation	ref	stem cell source[a]	material for stem cell culture[b]	differentiation	ref
rBMSCs	collagen I (3D culture, gel)	osteoblasts	193	hBMSCs	collagen I (3D culture, sponge)	chondrocytes	208
rat BMSCs	collagen I (3D culture, gel)	osteoblasts	105	rBMSCs	collagen I (3D culture, microsphere)	osteochondrocytes	209
hBMSCs	collagen I (3D culture, scaffold)	osteoblasts	202	hBMSCs	collagen I (3D culture, microsphere)	chondrocytes	210
rBMSCs	collagen I (3D culture, scaffold)	osteoblasts	183	bBMSCs	collagen I/alginate (3D culture, gel)	chondrocytes	91
hBMSCs	collagen I (3D culture, cross-linked scaffold)	osteoblasts	185, 190	rBMSCs	collagen I/alginate (3D culture, gel)	chondrocytes	211
hADSCs	collagen I (3D culture, electrospinning nanofiber)	osteoblasts	184	hBMSCs	collagen I/HA/PCL (3D culture, scaffold)	chondrocytes	151
hBMSCs	collagen I (3D culture, electrospinning nanofiber)	osteoblasts	182, 203	rat cardiac stem cells	collagen I/PLGA (3D culture, scaffold)	cardiomyocytes	212
rBMSCs	collagen I/PGA fiber (3D culture, sponge)	osteoblasts	144	mESCs	collagen I/Matrigel (3D culture, scaffold)	cardiomyocytes	213
rat BMSCs	collagen I/bioglass/PSN (3D culture, scaffold)	osteoblasts	204	mBMSCs	collagen I immobilized Sca-1 antibody (3D culture, scaffold)	cardiomyocytes	40
rBMSCs	collagen I/PGA (3D culture sponge)	osteoblasts	205	hBMSCs	collagen type I/PLCL (3D, electrospinning nanofiber)	neural cells	45
hBMSCs	collagen I/HYA (3D culture, scaffold)	osteoblasts	191	neural stem cells	collagen I (3D culture, grafting on elctrospinning mat)	neural cells	214
rBMSCs	collagen I/chitosan (3D culture, sponge)	osteoblasts	206	neural stem cells	collagen I (3D culture, gel)	neural cells	189
hBMSCs, Wharton's Jelly of UCB	collagen I/collagen III (3D culture, scaffold)	osteoblasts	34	rat neural stem cells	collagen I (3D culture, gel)	neural cells	217
rBMSCs	collagen I/chondroitin 6-sulfate (3D culture, scaffold)	osteoblasts, chondrocytes	56	mice neural stem cells	collagen I (3D culture, gel)	neural cells	215
hBMSCs	collagen I/HYA (3D culture, scaffold)	osteoblasts, chondrocytes	70	mice neural stem cells	collagen I/laminin (3D culture, gel), collagen I/fibronectin (3D culture, gel)	neural cells	215
pBMSCs	collagen I/PCL/TCP (3D culture, scaffold)	osteoblasts, adipocytes	197	rat stem cells	collagen I (3D culture, gel)	neuronal circuits	216
hBMSCs, hUCB-BMSCs	collagen I/collagen III (3D culture, gel)	osteoblasts, adipocytes	34	hBMSCs	fibroblast-embedded collagen I (3D culture gel)	epidermis	84
bBMSCs	collagen I (3D culture, gel)	chondrocytes	148	hADSCs	collagen II (3D culture, gel)	chondrocytes	71
hBMSCs	collagen I (3D culture, gel)	chondrocytes	63	bBMSCs	collagen II/aliginate (3D culture, gel)	chondrocytes	91
hADSCs	collagen I (3D culture, gel)	chondrocytes	71	rat BMSCs	atelocollagen (3D culture, honeycomb structure)	osteoblasts	110
mESCs	collagen I (3D culture, gel)	chondrocytes	207				

[a]ADSCs, adipose-derived stem cells; BMSCs, bone marrow stromal cells; ESCs, embryonic stem cells; hADSCs, human ADSCs; gBMSCs, goat BMSCs; hBMSCs, human BMSCs; mBMSCs, murine BMSCs; hESCs, human ESCs. [b]PCL, poly(ε-caprolactone); HYA, hydroxyapatite; PEG, polyethylene glycol.

scaffolds compared to 2D collagen coatings by day 21.[184] Extensive synthesis of mineralized extracellular matrix was observed on the nanofiber scaffolds assessed on day 21 with Alizarin Red staining. The results demonstrate that 3D nanoscale morphology plays a critical role in regulating cell fate determination and in vitro osteogenic differentiation of ADSCs under serum-free conditions.[184]

Chondrogenic differentiation of MSCs induced by collagen type I-based hydrogels has also been reported by several groups.[63,210,211,219] Chang et al. compared chondrogenesis of immortalized hBMSCs embedded in collagen type I gel to those grown in pellet culture.[219] The hBMSCs in collagen scaffolds expressed more glycosaminoglycan than those in pellet culture. Expression of the chondrogenic genes Sox9, aggrecan, collagen type II, and collagen type I (which indicates dedifferentiation) increased over time in pellet culture. However, only collagen type II and aggrecan expression in hBMSCs in the collagen gels increased over time, whereas Sox9 expression remained unchanged and collagen type I expression decreased, which indicated that there was no dedifferentiation from the chondrogenic lineage. These results indicate that chondrocytes differentiated from hBMSCs in collagen gel are superior to those generated in pellet culture because of their lower levels of dedifferentiation.

The regulation of ESCs in specific lineages of differentiation is a complex and technically challenging subject. Collagen type I microspheres encapsulated with mouse ESCs (mESCs) have been reported to be a suitable microenvironment for supporting mESCs and maintaining their undifferentiated state for a certain period.[207] However, Yeung et al. reported that the proportion of undifferentiated mESCs in the microspheres gradually decreased, and the proportion of MSCs was increased at later time points.[207] This result points to inductive properties of the collagen matrix for differentiating mESCs toward MSC lineages. It was reported that a lower initial collagen concentration facilitated the differentiation of mESCs into chondrogenic lineages, while mESCs differentiated into a more advanced stage of chondrocytes at a later time point using chondrogenic differentiation medium.[207] The cultivation of hESCs and human iPSC's in hydrogels or scaffolds of collagen type I or other ECM proteins and natural biopolymers could yield efficient differentiation into MSC

dx.doi.org/10.1021/cr3000169 | Chem. Rev. 2012, 112, 4507–4540

lineages, including osteoblasts, chondrocytes, and cardiomyocytes. This strategy would provide a larger-scale source of MSC lineage cells, which at present is limited to autologous patients.

Bioengineering complex tissues, which consist of multiple tissue phases with different structures and functions, is extremely challenging. In particular, it is difficult to create biological interfaces between mechanically dissimilar tissues such as cartilage and bone. The formation of the osteochondral interface with proper zonal organization is quite difficult, although tremendous efforts have been devoted to the developing osteochondral plugs.[209,220,221] An osteochondral interface is essential for preventing mechanical failure and maintaining normal function of cartilage.[209]

Cheng et al. demonstrated in vitro formation of a stem cell-derived osteochondral interface, with a calcified cartilage interface separating a noncalcified cartilage layer and an underlying bone layer, using BMSCs adhered to collagen type I microspheres.[209] Rabbit BMSCs were entrapped in collagen microspheres composed of a self-assembled nonfibrous meshwork.[209] BMSCs in the collagen microspheres were separated into two groups; one group was immersed in chondrogenic differentiation medium to drive differentiation into a chondrogenic lineage, whereas the other group was immersed in osteogenic differentiation medium and differentiated into an osteogenic lineage. Hundreds of cartilage-like and bonelike microspheres were aggregated to form chondrogenic and osteogenic layers, respectively.[209] Layers of these functional subunits were brought into contact with a central undifferentiated BMSC–collagen layer in a trilayered configuration for 3D cocultures. By 5 weeks, a calcified cartilage interface was formed between the noncalcified cartilage layer and the underlying bone layer. The cells at the interface region were found to be hypertrophic chondrocytes, and the extracellular matrix in this region contained collagen type II and type X, as well as calcium deposition. The osteochondral interface was reported to successively resemble the native osteochondral interface, based on the presence of hypertrophic chondrocytes, calcium phosphate deposits, collagen type II and type X, GAGs, and vertically aligned collagen bundles.[209] Thus, an osteochondral construct with proper zonal organization can be engineered using rabbit BMSCs and collagen in vitro.

Collagen type I hydrogels and scaffolds have also been used to promote differentiation of stem cells into neural cells. Ma et al. reported differentiation of central nervous system (CNS) mammalian stem cells into neuronal circuits in collagen type I hydrogels.[189] The proliferative capacity and differentiating potential of neural progenitors in 3D collagen gels suggest their potential use to promote neuronal regeneration.

5.2.2. Organic Hybrid Scaffolds of Collagen Type I.

The mechanical strength, swelling properties, and degradation behavior of scaffolds, as well as their biocompatibility, play crucial roles in the long-term performance of tissue-engineered stem cell/biomaterial constructs.[206,222–226] The shrinkage and weak mechanical strength of scaffolds present a serious problem for the use of purely collagen scaffolds in tissue engineering. Therefore, synthetic polymers or natural biopolymers are commonly blended into collagen scaffolds or hydrogels to enhance their mechanical strength (Table 8). No shrinking was observed in the scaffolds or hydrogels prepared from collagen blended with synthetic or natural biopolymers seeded with MSCs. Synthetic biopolymers, such as poly(L-lactic acid)-*co*-poly (3-caprolactone) (PLCL), poly(lactic-*co*-glycolic acid) (PLGA), and poly(glycolic acid) (PGA), and natural biopolymers of alginate, chitosan, and hyaluronic acid are blended with collagen for this purpose.

It should be noted that the contractile properties of skeletal cells are physiologically important, and the in vivo functions of contractility must be accounted for when developing tissue-formation strategies.[70,227,228] It was reported that a reduction in contraction induced by altering the cross-linking method of collagen–glycosaminoglycan scaffolds resulted in delayed collagen type II synthesis by articular chondrocytes.[229] Thus, malleable ECM proteins and synthetic biopolymers may provide environmental cues that direct cell differentiation, and these considerations should be included in scaffold design.

Fujita et al. prepared three kinds of scaffolds: a collagen type I sponge, a PGA–collagen type I sponge, and a PGA–collagen type I (UV) sponge seeded with rat BMSCs.[205] The PGA–collagen type I (UV) sponge was cross-linked by irradiation with UV light.[205] The collagen type I sponges with BMSCs shrank considerably, whereas PGA–collagen type I and PGA–collagen type I (UV) sponges maintained their original shapes. PGA–collagen type I sponges with and without cross-linking by UV induced high ALP activity (indicative of osteogenic differentiation) in medium containing the osteogenic supplement dexamethasone. The addition of bFGF together with dexamethasone promoted increased cell proliferation. However, extremely low osteogenic differentiation of BMSCs was found in collagen type I, PGA–collagen type I, and PGA–collagen type I (UV) sponges without osteogenic supplements in the culture medium.[205]

Osteoblasts were reported to maintain their phenotype and MSCs to undergo osteogenesis when cultured in ECMs containing collagen type I.[91,230,231] The interaction between collagen type I and $\alpha 2\beta 1$ integrin in MSCs, which was the major collagen type I receptor, was responsible for the osteoblastic differentiation of MSCs.[91,231]

Hybrid-type scaffolds made by a simple preparation method have also been reported. This collagen type I sponge can be formed in and on a mechanically strong PLGA knitted mesh. Dai et al. prepared three types of scaffolds (Figure 9): (i)

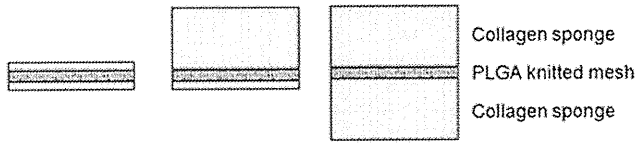

Figure 9. Schematic illustration of three structural designs of PLGA/collagen hybrid scaffolds. Black, PLGA knitted mesh; gray, collagen type I sponge. Modified with permission from ref 232. Copyright 2010 Elsevier Ltd.

collagen microsponges formed in the interstices of PLGA mesh; (ii) collagen microsponges formed on one side of PLGA mesh; (iii) collagen sponges formed on both sides of PLGA mesh.[232] All three groups of transplants showed homogeneous cell distribution, natural chondrocyte morphology, and abundant cartilaginous ECM deposition. Production of glycosaminoglycans and the expression of type II collagen and aggrecan mRNA were much higher in the collagen sponges formed on one or both sides of PLGA mesh than in the collagen sponges formed in interstices of the PLGA mesh. The engineered cartilage reached 54.8% (one side of PLGA mesh) and 49.3% (both sides of PLGA mesh) of the Young's modulus of native articular cartilage and 68.8% (one side) and 62.7%

dx.doi.org/10.1021/cr3000169 | *Chem. Rev.* 2012, 112, 4507–4540